Granger, J., Prokopenko, M. G., Sigman, D. M., Mordy, C. W., Morse, Z. M., Morales, L. V., Sambrotto, R. N., Plessen, B. (2011): Coupled nitrification-denitrification in sediment of the eastern Bering Sea shelf leads to 15N enrichment of fixed N in shelf waters. - Journal of Geophysical Research, 116, C11006

DOI: 10.1029/2010JC006751

Coupled nitrification-denitrification in sediment of the eastern Bering Sea shelf leads to ^{15}N enrichment of fixed N in shelf waters

J. Granger,[1] M. G. Prokopenko,[2] D. M. Sigman,[3] C. W. Mordy,[4] Z. M. Morse,[3] L. V. Morales,[3] R. N. Sambrotto,[5] and B. Plessen[6]

Received 22 October 2010; revised 10 August 2011; accepted 12 August 2011; published 5 November 2011.

[1] We studied the nitrogen biogeochemistry of the ice-covered eastern Bering Sea shelf using the isotope ratios ($^{15}N/^{14}N$ and $^{18}O/^{16}O$) of NO_3^- and other N species. The $^{15}N/^{14}N$ of late winter NO_3^- on the shelf decreases inshore and is inversely correlated with bottom water [NH_4^+], consistent with an input of low-$^{15}N/^{14}N$ NO_3^- from partial nitrification of NH_4^+ remineralized from the sediments. An inshore $^{15}N/^{14}N$ increase in total dissolved N (TDN) suggests that (1) the sediment-derived NH_4^+ is elevated in ^{15}N due to the same partial nitrification that yields the low-$^{15}N/^{14}N$ NO_3^-, and (2) ^{15}N-deplete NO_3^- from partial nitrification within the sediments is denitrified to N_2. The proportion of newly nitrified NO_3^- on the shelf, evidenced by an inshore decrease in NO_3^- $^{18}O/^{16}O$, is correlated with the N deficit, further implicating nitrification coupled to denitrification; however, a simple N isotope budget indicates a comparable rate of denitrification supported by diffusion of NO_3^- into the sediments. The isotopic impact of benthic N loss is further demonstrated by a correlation between the $^{15}N/^{14}N$ of shelf surface sediment and the N deficit of the overlying water column, both of which increase inshore and northward, as well as by Arctic NO_3^- isotope data indicating that the fixed N transported through Bering Strait has a $^{15}N/^{14}N$ higher than is found in the open Bering Sea. The significant net isotope effect of benthic N loss on the Bering shelf, 6–8 ‰, is at odds with previous assumptions regarding the global ocean's N isotope budget.

Citation: Granger, J., M. G. Prokopenko, D. M. Sigman, C. W. Mordy, Z. M. Morse, L. V. Morales, R. N. Sambrotto, and B. Plessen (2011), Coupled nitrification-denitrification in sediment of the eastern Bering Sea shelf leads to ^{15}N enrichment of fixed N in shelf waters, *J. Geophys. Res.*, *116*, C11006, doi:10.1029/2010JC006751.

1. Introduction

[2] The expansive continental shelf of the Bering Sea is characterized by a prolific ecosystem that is host to large populations of marine mammals and seabirds as well as to the largest U.S. fishery. The productivity of the shelf owes primarily to the high concentrations of nutrients that shoal onto the shallow continental shelf, fuelling strong seasonal blooms upon sea ice retreat. The production and export of algal material supports a thriving benthic shelf community. The escape of organic detritus down the adjacent continental slope leads to characteristic geochemical signals in the deep Bering Sea [e.g., *Lehmann et al.*, 2005] and may represent a significant mode of carbon transport into the ocean interior [*Walsh et al.*, 1985]. The Bering Sea shelf also serves as the gateway from the Pacific to the Arctic, and modifications of Pacific waters incurred from shelf processes affect the nutrient chemistry of the surface water column of the Arctic Ocean [*Cooper et al.*, 1999; *Jones et al.*, 2003; *Yamamoto-Kawai et al.*, 2006]. As with most high latitude systems, the Bering Sea shelf is undergoing changes in climate conditions that are altering its physical, chemical, and biological character [*Grebmeier et al.*, 2006; *Hunt et al.*, 2002]. However, the ultimate significance of these changes is unclear without an understanding of shelf processes, including their biogeochemistry.

[3] Productivity on the Bering shelf depends on the nutrient supply to the shelf water column. Shelf nutrient concentrations reach a maximum in late winter, when large expanses of the shelf are covered by sea ice, incident radiation is low, and the water column is mixed to the bottom. The spring phytoplankton bloom consumes these nutrients, resulting in a nutrient-poor upper mixed layer over the shelf from late spring to late summer [*Walsh and McRoy*, 1986]. Starting in the fall, nutrient concentrations throughout the water column increase in a "nearly linear fashion" through the winter until early spring [*Whitledge et al.*, 1986].

[1]Department of Marine Sciences, University of Connecticut, Groton, Connecticut, USA.
[2]Department of Earth Sciences, University of Southern California, Los Angeles, California, USA.
[3]Geosciences Department, Princeton University, Princeton, New Jersey, USA.
[4]Joint Institute for the Study of the Atmosphere and Ocean, University of Washington, Seattle, Washington, USA.
[5]Lamont-Doherty Earth Observatory, Earth Institute at Columbia University, Palisades, New York, USA.
[6]Geoforschungszentrum Potsdam, Potsdam, Germany.

0148-0227/11/2010JC006751

[4] Nutrient recharge during the winter months includes the exchange of nutrient-deplete shelf waters with nutrient-rich waters off the shelf, at least on the southern shelf [*Coachman and Walsh*, 1981; *Hansell et al.*, 1993; *Rho et al.*, 2005; *Sambrotto et al.*, 1986; *Stabeno et al.*, 2002a, 2007]. Exchange with the off-shelf water probably does not occur across the entire southern shelf [*Coachman*, 1986; *Coachman and Walsh*, 1981], such that nutrient recharge away from the shelf break is likely to occur at least partly through remobilization of nutrients from sediment [*Rowe and Phoel*, 1992; *Walsh and McRoy*, 1986; *Whitledge et al.*, 1986]. However, quantification of the relative and absolute rates of these processes is needed for the entire shelf.

[5] Reactive fixed N is particularly relevant in this context, as its concentration ratio relative to phosphate in waters entrained on-shelf from the open Bering Sea is 13, lower than an N/P of 16 for biological demand, assuming Redfield stoichiometry [*Lehmann et al.*, 2005]. On the Bering shelf, denitrification in sediment drives a further decrease in water column N/P both shoreward and northward [*Tanaka et al.*, 2004]. While there have been a number of studies of sedimentary denitrification on the Bering shelf [*Devol et al.*, 1997; *Haines et al.*, 1981; *Henriksen et al.*, 1993; *Koike and Hattori*, 1979; *Tanaka et al.*, 2004], further information is needed on its impact on N availability across the shelf. Because of transport through Bering Strait, N loss on the Bering shelf can also affect productivity in the Arctic. The Bering and Arctic shelves are responsible for a substantial fraction of the global benthic N loss, and are thus important in the global N budget [*Devol et al.*, 1997].

[6] In April of 2007 and 2008, as part of the Bering Ecosystem STudy (BEST), we collected samples at multiple stations on the eastern Bering Sea shelf, with a central goal of using the natural abundance isotopic composition of NO_3^- ($^{15}N/^{14}N$ and $^{18}O/^{16}O$) and other N species to uncover integrative constraints on the origins and fate of the fixed N in winter water which fuels the spring bloom. We sought to distinguish whether NO_3^- in the ice-covered water column is newly entrained from the shelf edge or remineralized directly from shelf sediment and to investigate the impact of benthic processes on the N distribution across the shelf. The data were interpreted with the help of a comprehensive set of ancillary hydrographic measurements collected as part of BEST. Our results provide new, more integrative confirmation that benthic processes are central to the burden of fixed N in the wintertime shelf water column. In particular, sediment recycling remobilizes fixed N into the water column, contributing substantially to the seasonal replenishment of NO_3^- in shelf waters. The NO_3^- isotopes point to coupled nitrification-denitrification in sediments as an important mechanism of fixed N loss on the shelf. We also find that coupled nitrification-denitrification in sediment communicates a ^{15}N-enrichment to water column fixed N, which has implications for the use of the N isotopes to reconstruct N budgets, on the Bering shelf and for the global ocean.

2. Study Area

[7] The eastern Bering Sea shelf is differentiated into three hydrographic domains: inner, middle, and outer shelf (Figure 1) [*Coachman*, 1986; *Schumacher and Kinder*, 1983]. The inner shelf is well mixed and relatively fresh, with salinities as low as 30.5 psu in April of 2007 and 2008, and is separated from the middle shelf by a front roughly coincident with the 50 m isobath [*Kachel et al.*, 2002; *Schumacher et al.*, 1979]. Waters in the inner shelf originate from the surface Alaska Coastal Current (ACC; salinity ~31.6), which enters the Bering Sea through the Aleutian Pass and meanders east and then northward inshore of the 50 m-isobath front as Alaska Coastal Water (ACW, Figure 1). ACW is further freshened by river discharge, predominantly from the Kuskokwim and Yukon Rivers. The middle shelf domain is delineated by two fronts at the 50 m and 100 m isobaths, and has a mean salinity of ~31.6, intermediate between inner and outer shelf regions [*Coachman and Charnell*, 1979]. It is mixed to the bottom in winter, due to convection from ice brines and/or intense wind mixing, and becomes two-layered in late spring from ice melt and solar insolation. The outer shelf domain extends from the 100 m isobath to the shelf break at 200 m depth [*Kinder and Coachman*, 1978]. It has a wind-mixed surface layer, a stratified transition layer, and a tidally mixed bottom layer contiguous with waters beyond the shelf break. Further north on the shelf, eastern shelf waters encounter more saline waters from the Anadyr region flowing eastward south of St-Lawrence Island toward the inner shelf (Figure 1) [*Coachman et al.*, 1975; *Danielson et al.* 2006; *Schumacher and Kinder*, 1983].

[8] The mean flow over the broad shelf is northward and generally slow, with monthly average estimates of flow of 1–6 cm sec^{-1} for ACW, ~1 cm sec^{-1} in the middle shelf domain, and 1–10 cm sec^{-1} along outer shelf [*Schumacher and Kinder*, 1983]. Water transport onto the shelf appears localized at discrete bathymetric canyons at the shelf break (Figure 1) [*Clement Kinney et al.*, 2009] and also occurs as a variable contribution of ACC waters entering at Unimak Pass [*Stabeno et al.*, 2002b]. On-shelf transport is mediated by episodic mesoscale eddies that do not appear to propagate inshore beyond the outer shelf region [*Mizobata et al.*, 2008; *Stabeno and Van Meurs*, 1999]. Exchange across the shelf hydrographic domains is reportedly mediated by tidally driven diffusion as well as by wind and buoyancy driven sub-tidal flows [*Coachman*, 1982, 1986; *Danielson et al.* 2011; *Hermann et al.*, 2002]. The magnitude and direction of cross-shelf fluxes, which affect the distribution of both conservative and non-conservative constituents, are both spatially and seasonally variable [*Danielson et al.*, 2011; *Reed*, 1998; *Stabeno et al.*, 2002a].

[9] Much of the eastern Bering Sea shelf is covered by sea ice in winter. In late fall, ice begins to form in the northern Bering Sea in polynyas on the leeward side of the coasts and islands. It is blown southward by the prevailing north-northeasterly winds, melts along the edge when infringing on warmer waters, and extends to or beyond the Pribilof Islands [see *Stabeno et al.*, 2007]. The growth of sea ice leaves behind salty waters in seasonal polynyas due to brine rejection, whereas ice melt in spring results in freshwater lenses that contribute to the formation of a stratified mixed layer over the middle and outer shelf.

3. Sample Set and Measurements

[10] We collected samples on two cruises as part of the Bering Ecosystem Study (BEST) in April of 2007 and 2008,

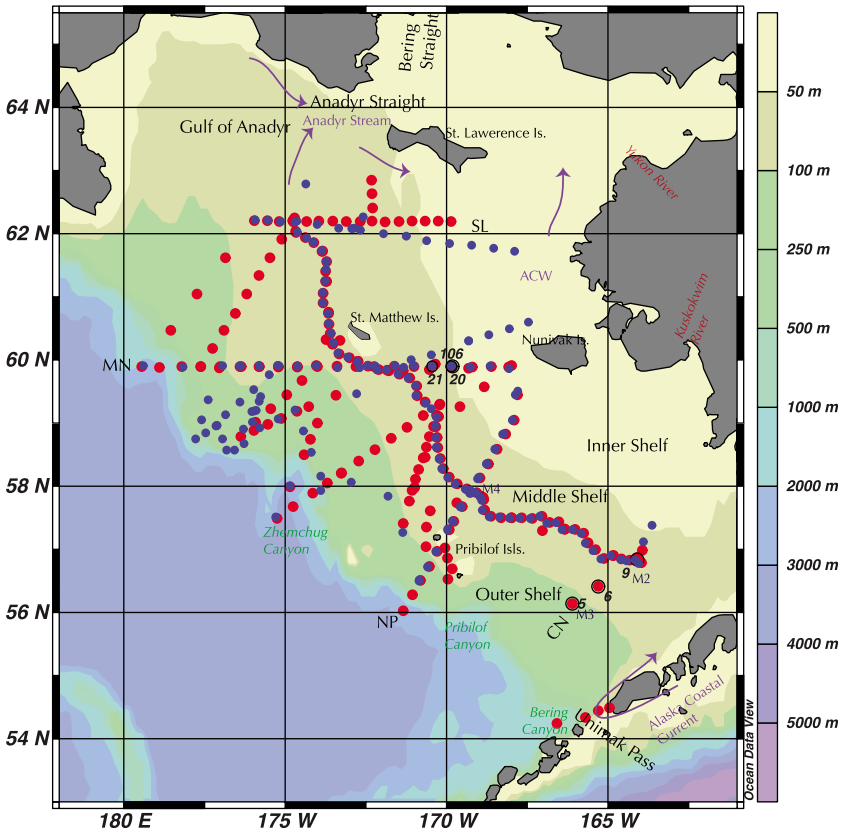

Figure 1. Cruise tracks during HLY-07-01 (blue) and HLY-08-02 (red). Note the location of hydrographic lines and mooring locations: CN (Canyon-Nunivak), 70-m-isobath, NP (Nunivak-Pribilof), MN (St. Matthew-Nunivak), SL (St. Lawrence), and the location of the M2, M3 and M4 moorings. Map generated with Ocean Data View (R. Schlitzer, 2002, http://www.awi-bremerhaven.de/GEO/ODV).

aboard the icebreaker *U.S.C.G. Healy* (HLY-07-01 and HLY-08-02). Discrete hydrographic lines extending on- and off-shelf (CN, NP, MN, SL, 70 m isobath; Figure 1) were visited in both years, along with additional stations that were visited in only one of the two years. Sea ice covered many of the shelf stations, with ice cover extending over the middle shelf down to ~58°N in 2007 and further, to the shelf edge and beyond the Pribilofs in 2008 (Figure S1 in Text S1 in the auxiliary material).[1]

[11] Hydrographic measurements were made using a conductivity-temperature-depth profiler (CTD), equipped with a transmissometer and a fluorometer. In situ fluorescence was converted to chlorophyll-*a* concentrations from an empirical calibration with discrete measurements of water column chlorophyll-*a* concentrations (M. Lomas, HLY0802 chlorophyll and primary production [Lomas/BIOS], 2010, http://data.eol.ucar.edu/codiac/dss/id=102.136, and J. Napp, Spring chlorophyll concentrations on the eastern Bering Sea shelf, 2007, http://data.eol.ucar.edu/codiac/dss/id=102.079). Seawater was collected from an attached rosette of 24 Niskin water collection bottles. Salinity-calibration samples were collected at all stations and analyzed on board with a salinometer. Nutrients (NO_3^-, NO_2^-, PO_4^{3-}, $Si(OH)_4$, NH_4^+) were analyzed directly on board with Technichon II autoanalyzer using standard methods [*Gordon et al.*, 1994; *Mantoura and Woodward*, 1983]. Dissolved oxygen was determined on board by Winkler titrations [*Carpenter*, 1965]. Surface sediment samples were collected at some stations on the shelf in April 2008 with a vanVeen grab. The top 2 cm of the sediment column was stored frozen for later isotopic analysis.

[12] Seawater samples for NO_3^- isotope analyses were prefiltered though a 0.2 μm PES (polyether sulfone) membrane into 60 mL HDPE (high density polyethylene) bottles and were stored frozen until analysis. NO_2^- was removed with sulfamic acid [*Granger and Sigman*, 2009] in the few samples where nitrite comprised ≥5% of the sum of NO_3^- plus NO_2^-. The $^{15}N/^{14}N$ and the $^{18}O/^{16}O$ of nitrate were analyzed by the 'denitrifier method' [*Casciotti et al.*, 2002; *Sigman et al.*, 2001]. Briefly, 20 nmoles of nitrate are quantitatively reduced to N_2O by denitrifying bacteria that lack an active terminal N_2O reductase. The product N_2O was analyzed by continuous flow isotope ratio mass spectrometry on a Thermo-Finnigan Delta Plus IRMS. Isotope ratios are reported in delta notation (δ) in units of per mil (‰):

$$\delta^{15}N(‰) = \left(^{15}N/^{14}N_{sample}/^{15}N/^{14}N_{standard} - 1\right) \times 1000, \text{ and}$$

$$\delta^{18}O(‰) = \left(^{18}O/^{16}O_{sample}/^{18}O/^{16}O_{standard} - 1\right) \times 1000$$

[1] Auxiliary materials are available in the HTML. doi:10.1029/2010JC006751.

[13] The $^{15}N/^{14}N$ reference is N_2 in air, and the $^{18}O/^{16}O$ reference is Vienna Standard Mean Ocean Water (VSMOW). Individual analyses were referenced to injections from a laboratory standard N_2O tank and standardized using the nitrate reference material IAEA-N3 (4.7‰ versus N_2 and 25.6‰ versus SMOW [*Böhlke et al.*, 2003; *Gonfiantini et al.*, 1995]), and USGS-34 (−1.8‰ versus N_2; −27.9‰ versus SMOW [*Böhlke et al.*, 2003]). Samples were analyzed at least in duplicate, yielding an average standard deviation of 0.3‰ for N and 0.5‰ for O.

[14] The $\delta^{15}N$ of total dissolved N (TDN) was measured in water samples collected at discrete depths at a few shelf stations sampled in 2007, by peroxidation of TDN to NO_3^- followed by N isotope analysis with the denitrifier method [*Knapp et al.*, 2005]. [TDN] was quantified as $[NO_3^-]$ by reduction to NO in heated vanadium solution followed by chemiluminescence detection on a Teledyne 200E Chemiluminescence NOx analyzer [*Braman and Hendrix*, 1989].

[15] Surface sediment samples were freeze-dried and homogenized. Replicated sub-samples were allotted into pre-combusted tin capsules. Stable N isotope analysis was performed by combustion on a high temperature elemental analyzer (Carlo Erba NCS 2500) interfaced with a continuous flow IRMS (Delta Plus XL). Analyses were calibrated with recognized standards, IAEA-N1 ($\delta^{15}N$ = 0.4‰) and IAEA-N2 ($\delta^{15}N$ = 20.3‰). Instrumental precision was 0.3‰.

4. Results

4.1. Nitrate Concentrations on the Shelf

[16] The concentration of NO_3^- ($[NO_3^-]$) in 'winter water' throughout the shelf was similar in both years, as gauged from bottom water $[NO_3^-]$ accrued on the shelf by April of each year (Figures 2a and 2b). The $[NO_3^-]$ off-shelf at depths of 150 to 200 m was ≥25 μM, gradually decreasing eastward along the bottom layer of the outer shelf, reaching 20 μM at the front delineated by the 100 m isobath. On the middle shelf, bottom water $[NO_3^-]$ ranged between 10 μM and 15 μM in both years, whereas the inner shelf had the lowest observed bottom water $[NO_3^-]$, averaging ≤5 μM. The pattern of decreasing $[NO_3^-]$ from off-shelf to inshore is consistent with previous surveys of winter water nutrients [*Rho et al.*, 2005; *Whitledge et al.*, 1986]. This primarily reflects the mixing of NO_3^--poor ACW inshore with NO_3^--rich waters at the shelf break, as is also evident from the analogous distributions of phosphate (PO_4^{3-}) and silicic acid ($Si(OH)_4$) (Figure S2 in Text S1).

[17] While bottom water $[NO_3^-]$ was similar between years, stations with a fresher shallow mixed layer along the retreating ice edge showed clear surface NO_3^- depletion due to algal growth, particularly in 2007 (Figures S2 and F3 in Text S1). Coincident depletions of PO_4^{3-} and $Si(OH)_4$, as well as maxima in the concentrations of O_2 and chlorophyll-*a*, provide confirmation of ongoing or recent biological NO_3^- drawdown (Figure S3 in Text S1). In April 2007, there was also evidence of biological NO_3^- drawdown at stations under ice at the inner shelf and along the SL line, whereas biological NO_3^- utilization at ice-covered stations was much less prevalent in 2008 (Figure S2 in Text S2).

4.2. Ammonium Concentrations on the Shelf

[18] Shelf waters had significant concentrations of ammonium (NH_4^+) in both years (Figures 2c and 2d). The lowest NH_4^+ concentrations were measured in the outer shelf (≤0.5 μM), whereas concentrations ranged between 0.5 and 3 μM in the middle shelf and reached as high as 4 μM in the inner shelf. The distribution of NH_4^+ in shelf waters was comparable in both years, albeit lower at the inner shelf off Nunivak Island in 2007, likely due to algal growth as evidenced by elevated chlorophyll-*a* and O_2 concentrations (Figure S3 in Text S1). Concentrations were typically higher near the sediment-water interface, even in well-mixed water columns, indicating that NH_4^+ was being released from the sediment (Figure S3 in Text S1). The concentration of nitrite (NO_2^-) throughout the shelf was modest in both years, consistently <0.7 μM (data not shown).

4.3. N Deficit on the Shelf

[19] We quantify the concentration of fixed N lost relative to $[PO_4^{3-}]$ with the tracer N* defined as N* (μM) = $([NO_3^-] + [NO_2^-] + [NH_4^+]) - 16*[PO_4^{3-}] + 2.9$ (Figures 2a, 2f, and 3) [*Gruber and Sarmiento*, 1997]. The N* at Unimak Pass, a throughflow of the ACC that feeds the inner shelf region, is similar to that of off-shelf surface water from the open Bering Sea. Similarly, Anadyr waters are entrained up slope from the shelf break [*Nihoul et al.*, 1993], and are thus characterized by the same initial N* as Bering shelf waters. Thus, most of the on-shelf N* variation likely derives from in situ biogeochemical processes. Since the Bering shelf water column is oxygenated, the observed decreases in N* from off-shelf values are likely dominated by benthic denitrification. The Yukon River is reportedly highly oligotrophic [*Guo et al.*, 2004], as is probably the Kuskokwim River, such that their waters would have a N* of ~2.9 μM by our definition and would thus increase the N* of shelf water.

[20] Relative to the off-shelf waters, stations along the outer-shelf showed a modest decrease in N*, which ranged between −3 and −6 μM south of the MN line, and reached −8 μM in both years at outer shelf stations north of the MN line (Figures 2e and 2f). The inorganic N loss recorded in waters overlying the middle and inner shelf regions was greater than that at corresponding latitudes on the outer shelf, with N* between −6 μM and −9 μM on the southern portion of the shelf. Directly north of 58°N, both middle and inner shelf regions showed evidence of considerable inorganic N loss relative to P, with N* values reaching −11 μM. At the northernmost latitudes between 59°N and 60°N, the middle and inner shelf regions also recorded N* values as low as −13 μM. Thus, the characteristic decrease in $[NO_3^-]$ observed across the shelf (Figure 2) is strengthened by sedimentary N loss, which becomes increasingly pronounced inshore and northward.

4.4. The $\delta^{15}N$ of NO_3^-

[21] The $\delta^{15}N$ of NO_3^- ($\delta^{15}N_{NO3}$) was ~5.6‰ at 2500 m off-shelf, at a concentration of ~40 μM (Figures 3 and 4a), as observed previously [*Lehmann et al.*, 2005]. In the thermocline of the open Bering Sea, below the wind-mixed winter layer (at a specific density of 26.5 mg cm^{-3}, between

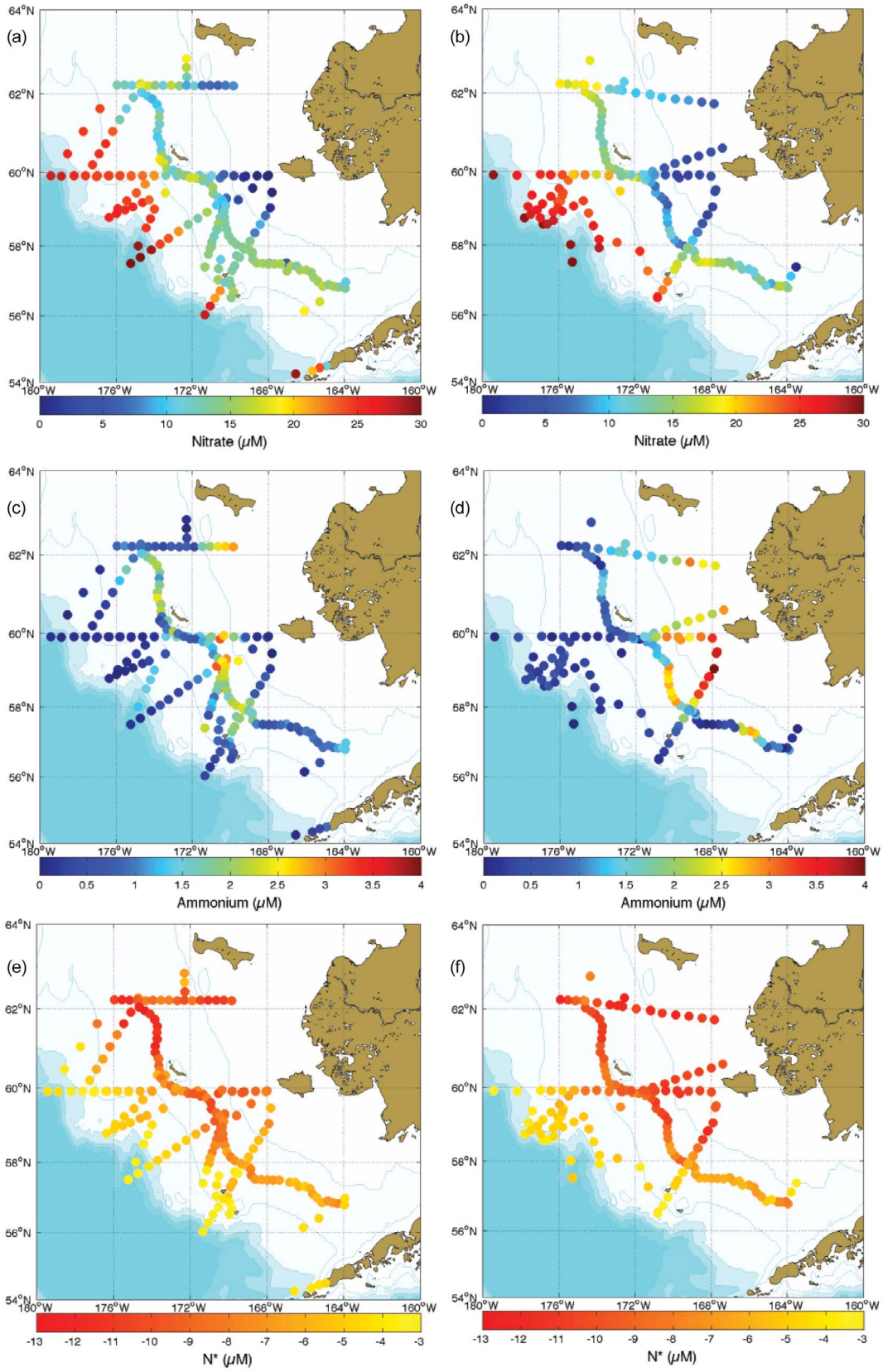

Figure 2. Chemical properties of the water-column along hydrographic cruise lines on the eastern Bering Sea shelf in April 2007 and 2008. (a, b) $[NO_3^-]$ at bottom water depths to 200 m in 2007 and 2008. (c, d) $[NH_4^+]$ at bottom water depths to 200 m. (e, f) N* at bottom water depths to 200 m. N* (μM) = $[NO_3^-]$ + $[NO_2^-]$ + $[NH_4^+]$ − 16 * $[PO_4^{3-}]$ + 2.9.

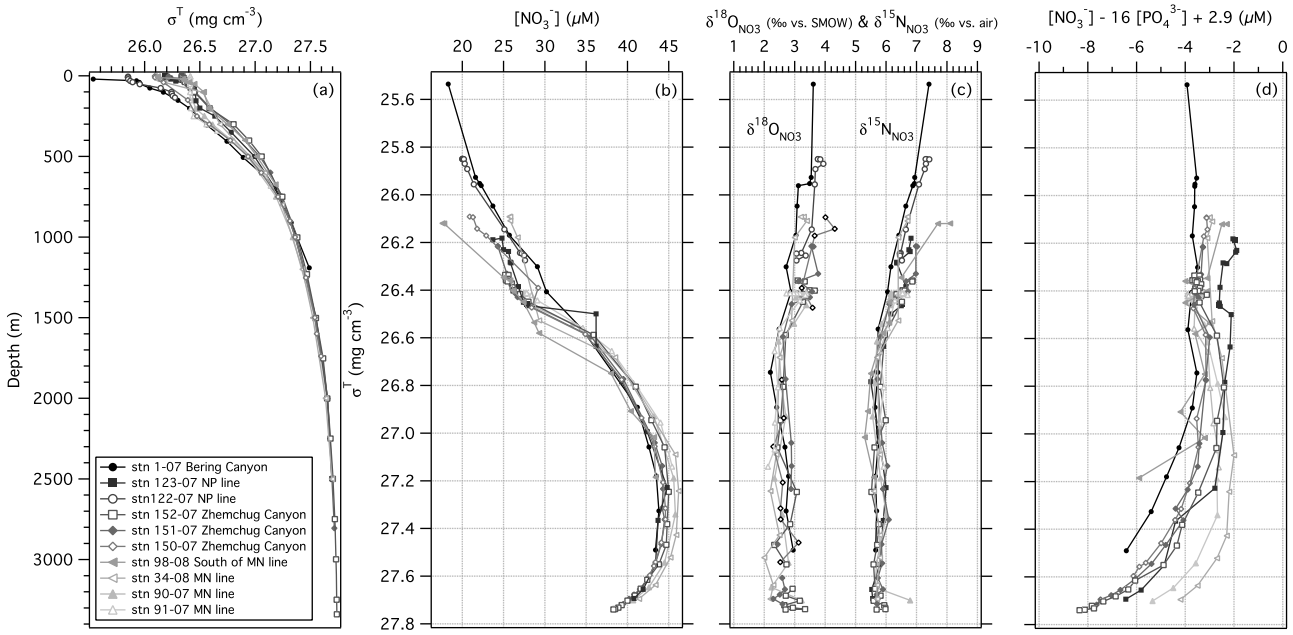

Figure 3. Physical and chemical properties of the water column at deep stations off the eastern Bering Sea shelf in April 2007 and 2008. (a) Depth profiles of the specific density. Isopycnal profiles of (b) $[NO_3^-]$, (c) the $\delta^{15}N$ and $\delta^{18}O$ of NO_3^-, and (d) the NO_3^- deficit relative to PO_4^{3-}.

150 and 300 m, depending on the station), $[NO_3^-]$ was ~28 μM and $\delta^{15}N_{NO3}$ was ~6‰. Toward the surface, $\delta^{15}N_{NO3}$ was either (1) homogeneous throughout the deep winter mixed layer, averaging 6.3‰ at a $[NO_3^-]$ of ~25 μM, or (2) showed increasing $\delta^{15}N_{NO3}$ toward the surface–up to 8‰ at the surface in one profile–with concurrently decreasing $[NO_3^-]$. The off-shelf stations showing structure in $[NO_3^-]$ and $\delta^{15}N_{NO3}$ were characterized by a gradual halocline contiguous with fresher shelf waters (Figure 3).

[22] Over the outer shelf region, $\delta^{15}N_{NO3}$ was similar to off-shelf values at corresponding depths, averaging 6.5‰ in bottom waters between 200 and 100 m (Figure 4a). Toward the surface over the outer shelf, $\delta^{15}N_{NO3}$ generally increased with incident nitrate consumption due to phytoplankton growth in marginal ice zones, as indicated by proportional increases in the concentrations of O_2 and chlorophyll-*a* (Figure 4b and Figure S3 in Text S1). This is consistent with N isotope discrimination during algal NO_3^- assimilation. $\delta^{15}N_{NO3}$ upwards of 20‰ was associated with nearly complete NO_3^- consumption in marginal ice blooms over the outer shelf and the southern middle shelf, particularly in 2007 (Figure S3 in Text S1). Conversely, in ice-covered shelf waters without recent algal growth, $\delta^{15}N_{NO3}$ showed a tendency toward low values (≤3‰) at lower $[NO_3^-]$, particularly at the inner shelf and along the northernmost SL line.

4.5. The $\delta^{18}O$ of NO_3^-

[23] The $\delta^{18}O$ of nitrate ($\delta^{18}O_{NO3}$) showed patterns similar to those observed for $\delta^{15}N_{NO3}$ (Figures 3 and 4c). Deep-water $\delta^{18}O_{NO3}$ in the open Bering Sea was ~2.2‰, increasing to ~2.9‰ below the winter mixed layer. Values were ~3.2‰ throughout the deep mixed winter layer, or reached up to 3.5‰ at the surface at more stratified stations off-shelf. On the outer shelf, $\delta^{18}O_{NO3}$ averaged 3.2‰ at bottom depths and increased congruently with NO_3^- depletion, reaching ≥20‰ in marginal ice blooms. On the middle and inner shelf regions south of the Pribilof Islands, marginal ice zones also showed correspondingly elevated $\delta^{18}O_{NO3}$. As with $\delta^{15}N_{NO3}$, ice-covered waters not demonstrably influenced by recent algal growth recorded lower $\delta^{18}O_{NO3}$ at lower $[NO_3^-]$, as low as −1‰ in the inner shelf.

4.6. The $\delta^{15}N$ of Surface Sediment

[24] The $\delta^{15}N$ of surface sediment ($\delta^{15}N_{sed}$) on and off-shelf ranged between 5.3‰ and 10.4‰ (Figure 5). The lower end of this range was observed at off-shelf stations, from 5.3‰ north of Bering Canyon to 6.4‰ at Zhemchug Canyon. Along the outer shelf region, the $\delta^{15}N_{sed}$ ranged between 6‰ and 7‰ and increased inshore, to ~8‰ and ~9‰ in the middle and inner shelf regions, respectively, and as high as 10.4‰ along the SL line leeward of St-Lawrence Island.

5. Interpretation and Discussion

5.1. Remobilization of N From Sediment in Shelf Winter Waters

[25] The $\delta^{15}N$ of nitrate ($\delta^{15}N_{NO3}$) provides insight into the origin and fate of fixed N in 'winter water' on the shelf. Given two null hypotheses: (1) exchange with off-shelf waters during winter months is the primary mechanism of NO_3^- recharge of the shelf water column, and (2) any N loss to sedimentary denitrification throughout the winter months does not impart ^{15}N-enrichment to NO_3^- in the overlying water column [*Brandes and Devol*, 1997], the $\delta^{15}N_{NO3}$ throughout the shelf is expected to reflect largely that of NO_3^- off-shelf–with the exception of regions and periods of recent algal growth, where the $\delta^{15}N_{NO3}$ should be elevated relative to the off-shelf NO_3^- supply.

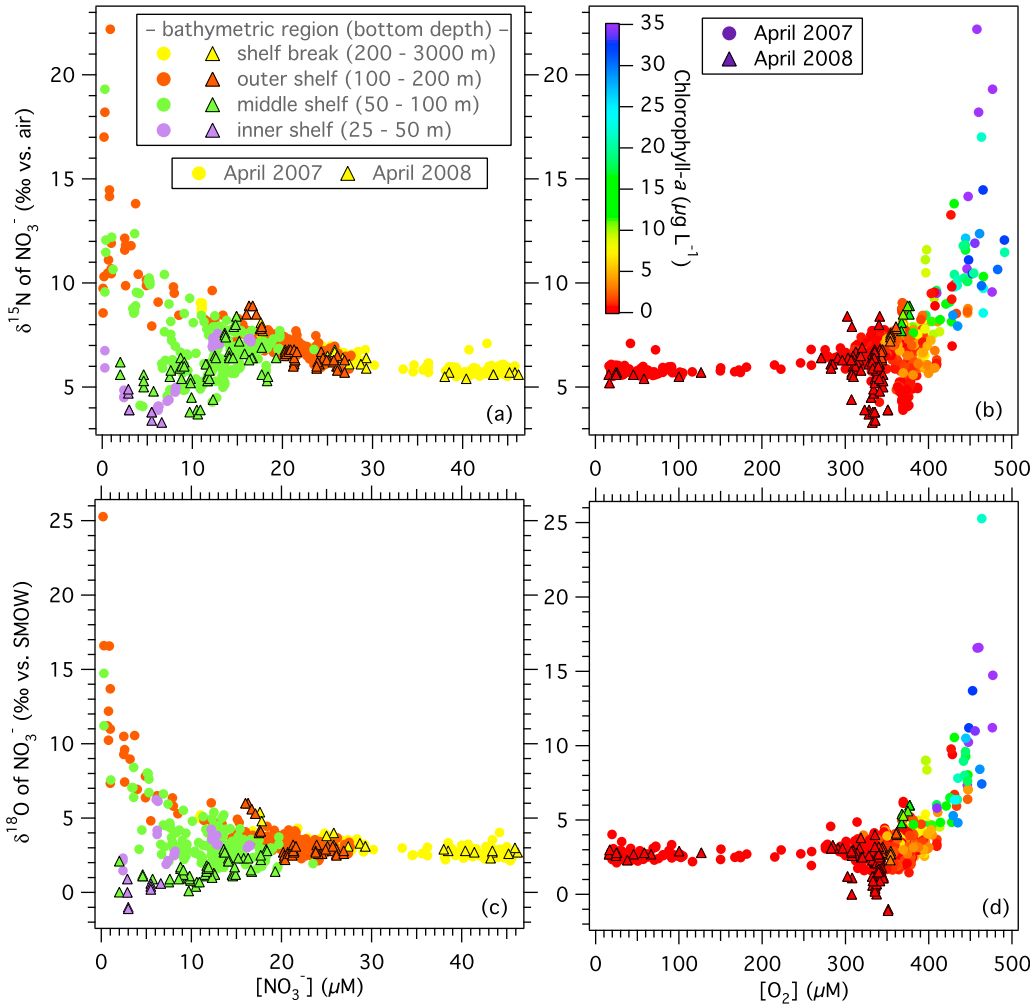

Figure 4. The $\delta^{15}N$ and the $\delta^{18}O$ of NO_3^- on the eastern Bering Sea shelf in April 2007 and 2008. (a) The $\delta^{15}N_{NO3}$ versus $[NO_3^-]$ per hydrographic region of the Bering shelf. (b) The $\delta^{15}N_{NO3}$ versus O_2 concentration per corresponding chlorophyll-*a* concentration. (c) The $\delta^{18}O_{NO3}$ per $[NO_3^-]$ hydrographic region of the Bering shelf. (d) The $\delta^{18}O_{NO3}$ versus O_2 concentration per corresponding chlorophyll-*a* concentration.

[26] In outer shelf waters where algal growth was not evident, the $\delta^{15}N_{NO3}$ was predictably similar to that off-shelf (Figure 4). However, the $\delta^{15}N_{NO3}$ recorded in the inner and middle shelf regions, notwithstanding regions bearing evidence of recent algal growth, tended toward lower values, as low as ~3‰ (Figure 4). The amplitude of the $\delta^{15}N_{NO3}$ appeared to be associated with bottom depth, as the lowest $\delta^{15}N_{NO3}$ was observed inshore and near St-Lawrence Island. The NO_3^--deplete rivers discharging at the Alaskan coast are unlikely to generate this isotopic signal [*Guo et al.*, 2004]. Rather, the association of the $\delta^{15}N_{NO3}$ with bottom depth suggests that low ^{15}N NO_3^- in winter water is generated locally from sedimentary processes. Nitrogen fixation, which generates newly fixed N with a $\delta^{15}N$ of −2–0‰ [*Hoering and Ford*, 1960], is a possible sedimentary source [*Fulweiler et al.*, 2007]; however, it would counter the N* decrease toward the coast. A more parsimonious explanation for the low $\delta^{15}N_{NO3}$ is the partial oxidation of NH_4^+ released from sediment. Indeed, the concentration of NH_4^+ throughout the shelf offers the best correlate to the $\delta^{15}N_{NO3}$, with lower $\delta^{15}N_{NO3}$ coinciding with higher $[NH_4^+]$ (Figure 6). NH_4^+ in sediment is generated by the ammonification of organic material and is released by diffusive and non-diffusive processes [*Glover and Reeburgh*, 1987; *Lomstein et al.*, 1989; *Ray et al.*, 2006; *Rowe and Phoel*, 1992; *Whitledge et al.*, 1986]. The $\delta^{15}N$ of NH_4^+ ($\delta^{15}N_{NH4}$) produced by ammonification in sediment is expected to be similar to that of the organic N substrate, assuming little diagenetic offset between the organic N substrate and the ammonia product [*Prokopenko et al.*, 2006; *Velinsky et al.*, 1991]. A substantial organism-level N isotope effect of ≥14‰ is expected during the oxidation of NH_4^+ to NO_2^-, as documented in culture studies of ammonia oxidizing bacteria [*Casciotti et al.*, 2003]. Because there is no significant accretion of NO_2^- in the water column, NH_4^+ oxidation appears to be the rate-determining step during the oxidation of NH_4^+ to NO_3^-, causing the partial nitrification of NH_4^+ to NO_3^- that is at least ~14‰ lower than the NH_4^+.

[27] The incidence of ^{15}N-deplete NO_3^- was documented previously at three stations on the southern shelf in August 2001, where the $\delta^{15}N_{NO3}$ measured below the surface mixed layer ranged from 3.9 to 5.2‰ [*Tanaka et al.*, 2004]. The

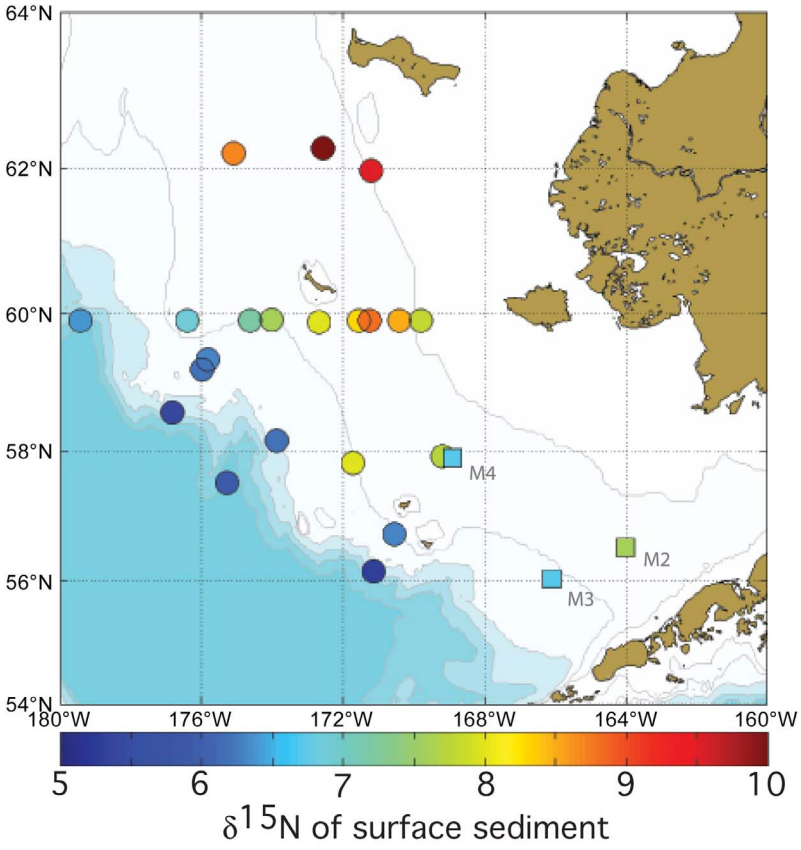

Figure 5. The $\delta^{15}N$ of surface sediment ($\delta^{15}N_{sed}$) on the eastern Bering shelf in April 2008 (circles), and in May 1998 (squares; [*Smith et al.*, 2002]).

slight depletion in $\delta^{15}N_{NO3}$, with respect to oceanic deep waters (taken as 5‰), was tentatively ascribed to new NO_3^- input from in situ nitrification. Similarly, on the western Washington shelf, the $\delta^{15}N_{NO3}$ in waters overlying sediment core incubations became progressively ^{15}N-deplete, which was attributed to the partial nitrification of NH_4^+ released from sediment [*Hartnett*, 1998].

[28] Our observation of ^{15}N-deplete NO_3^- over the Bering shelf provides evidence that sedimentary remobilization contributes to the water column NO_3^- inventory and becomes increasingly important away from the shelf edge. This is consistent with the expectations that seasonal exchange with waters off-shelf does not result in whole sale renewal of shelf waters [*Coachman and Walsh*, 1981] and that recycling of organic matter in sediment is a substantial source of nutrients to the water column in more quiescent parts of the shelf. Previous studies estimated that ~10% of the NO_3^- consumed by primary production during the summer originates from NH_4^+ released from sediment at the current location of the M2 mooring on the southern shelf (Figure 1) [*Rowe and Phoel*, 1992; *Whitledge et al.*, 1986]. The $\delta^{15}N_{NO3}$ measurements presented here convey that sediment remobilization of inorganic N is important to seasonal nutrient recharge, but it is difficult to provide quantitative constraints on the relative contribution of regenerated N to seasonal recharge solely from the $\delta^{15}N_{NO3}$. The amplitude of the isotope effect associated with ammonia oxidation covers a potentially broad range, from 14–35‰ among strains

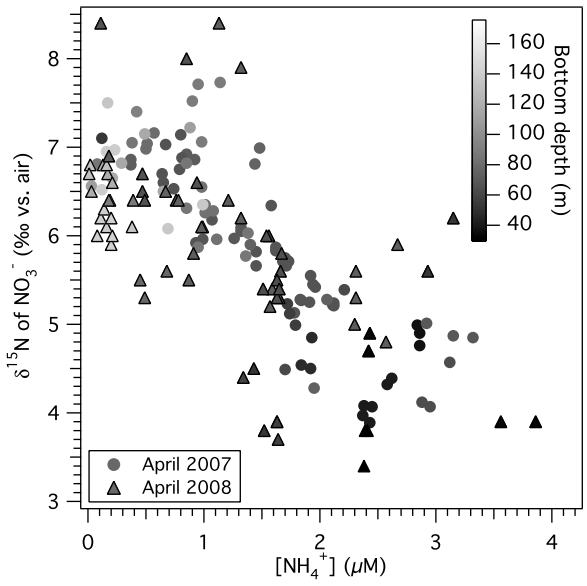

Figure 6. The $\delta^{15}N_{NO3}$ versus $[NH_4^+]$ per bottom depth in April 2007 and April 2008 on the eastern Bering Sea shelf. The data are restricted to samples bearing limited evidence of recent or incident phytoplankton growth (chlorophyll-*a* concentration ≤1.6 μg L^{-1}; $[O_2] \leq 380$ μM).

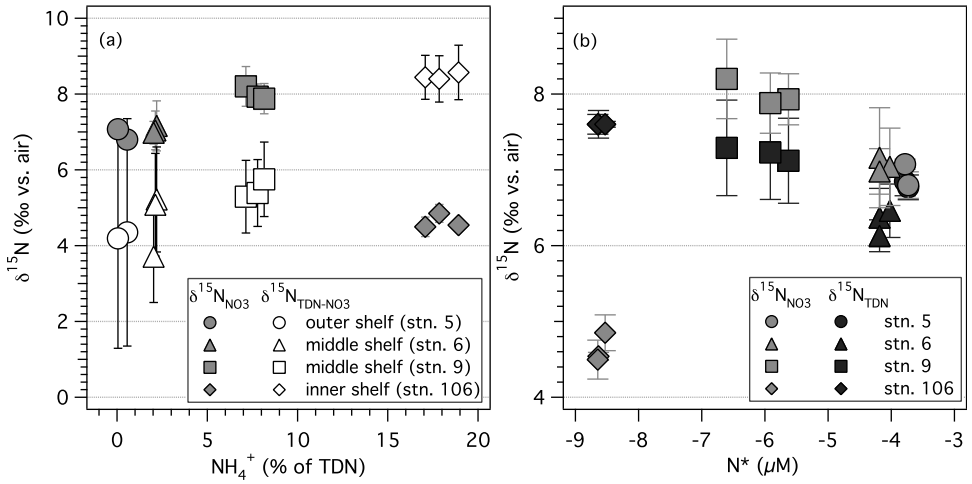

Figure 7. (a) The δ^{15}N of TDN - NO_3^- (±1 σ) versus the % of TDN as NH_4^+ in the bottom layer at five hydrographic stations on the eastern Bering shelf visited in April 2007 (see Figure 1). (b) The δ^{15}N of TDN (±1 σ) versus N* in the bottom layer at four hydrographic stations. The error terms (1 σ) associated with the derived measurements of the $\delta^{15}N_{TDN\text{-}NO3}$ were compounded from the respective measurement errors of [TDN], $\delta^{15}N_{TDN}$, $\delta^{15}N_{NO3}$, as well as a conservative error estimate of 5% for [NO_3^-].

examined in culture studies [*Casciotti et al.*, 2003]. Moreover, the $\delta^{15}N_{NO3}$ of NO_3^- produced by nitrification will converge on that of the NH_4^+ substrate when the latter is completely oxidized; thus, the contribution of regenerated NO_3^- relative to that newly delivered from the shelf edge cannot be differentiated the on basis of their respective $\delta^{15}N_{NO3}$. Nevertheless, the ^{15}N signal of benthic N recycling observed in the water column implies that sediment remobilization is important to wintertime nutrient recharge, even if conservative assumptions are made regarding the inherent ^{15}N dynamics of nitrification.

[29] A more quantitative tracer of N recycling is provided by the $\delta^{18}O_{NO3}$. The $\delta^{18}O_{NO3}$ is directly sensitive to the extent of nitrification, which reflects the δ^{18}O of ambient water ($\delta^{18}O_{H20}$). Based on the results of *Sigman et al.* [2009], we estimate that $\delta^{18}O_{NO3} \sim \delta^{18}O_{H20} + 1‰$. Measurements of the $\delta^{18}O_{NO3}$ in winter water show a progressive decrease from the shelf edge to shallow water depths, from ~3.2‰ at the shelf edge to as low as −1‰ at the inner shelf (Figure 4c). These observations support the notion that NO_3^- is increasingly regenerated away from the shelf edge, as implied by the $\delta^{15}N_{NO3}$. Specifically, the negative $\delta^{18}O_{NO3}$ at the inner shelf, where the $\delta^{18}O_{H20}$ of seawater seasonally reaches as low as −2‰ due to continental run-off [*Cooper et al.*, 1999; *Grebmeier et al.*, 1990], suggest that 100% of the NO_3^- in the water column inshore has been regenerated from organic matter rather than imported from the shelf break. The dynamics of the $\delta^{18}O_{NO3}$ in relation to the $\delta^{18}O_{H2O}$ will be considered explicitly in a later manuscript (J. Granger et al., manuscript in preparation, 2011).

5.2. ^{15}N-Enrichment of NH_4^+ by Nitrification

[30] If ^{15}N-deplete NO_3^- derives from partial nitrification, then the residual pool of NH_4^+ must be enriched in ^{15}N relative to the organic N being remineralized. The ^{15}N-enrichment of ambient NH_4^+ could be established directly with measurements of the $\delta^{15}N_{NH4}$, which we are undertaking in ongoing work. In the meantime, measurements of the δ^{15}N of total dissolved nitrogen (TDN) on the shelf suggest that NH_4^+ is ^{15}N-enriched relative to the co-incident $\delta^{15}N_{NO3}$: The reduced fixed N pool (TDN–NO_3^-) tended to higher δ^{15}N at stations where NH_4^+ comprised a relatively larger fraction of the total dissolved N pool (Figure 7a). The $\delta^{15}N_{TDN\text{-}NO3}$ admittedly subsumes both the $\delta^{15}N_{NH4}$ and the δ^{15}N of dissolved organic nitrogen ($\delta^{15}N_{DON}$), such that the $\delta^{15}N_{NH4}$ cannot be derived exclusively from the difference of $\delta^{15}N_{TDN}$ and $\delta^{15}N_{NO3}$. However, the concentration of DON was similar among the few stations surveyed (Figure S4 in Text S1). Moreover, DON delivered by rivers, which could be hypothesized to account for the increase in the δ^{15}N of TDN inshore, is relatively ^{15}N-deplete, ≤0‰ year-round [*Guo and Macdonald*, 2006], which would act to decrease δ^{15}N TDN, in the opposite sense of the observations. Thus, the ^{15}N-enrichment of $\delta^{15}N_{TDN\text{-}NO3}$ at stations with greater proportional NH_4^+ is most likely imposed by the $\delta^{15}N_{NH4}$, which is ^{15}N-enriched from partial nitrification occurring in the water column and in surface sediment. Assuming a conservative δ^{15}N of 5‰ for DON inshore, akin to that off-shelf (Figure S4 in Text S1), a corresponding value for $\delta^{15}N_{NH4}$ is obtained from the weighted contributions of N species to the TDN mass balance: For example, given 10.6 μM TDN with a $\delta^{15}N_{TDN}$ = 7.6‰, and 2.4 μM NO_3^- with a $\delta^{15}N_{NO3}$ = 4.4‰, the $\delta^{15}N_{NH4}$ of the ambient 1.9 μM NH_4^+ is on the order of ~20‰ (station 106; Figure 7b and Figure S4 in Text S1). Interestingly, the δ^{15}N of plankton net tow material (≤150 μm) collected from the ice-covered water column in April 2007 and 2008 was also elevated, between 10‰ and 17‰, which may reflect assimilation of regenerated N sources by phytoplankton in the ice-covered water column, thus also arguing for a relatively elevated $\delta^{15}N_{NH4}$ (L. Morales et al., unpublished manuscript, 2011).

5.3. N Loss From Coupled Nitrification-Denitrification in Sediment

[31] In contrast to the $\delta^{15}N_{NO3}$, the $\delta^{15}N_{TDN}$ measured at a few stations cross shelf was more ^{15}N-enriched inshore ($\delta^{15}N_{TDN}$ = 7.6‰ at station 106) than at stations off-shelf ($\delta^{15}N_{TDN}$ = 6.2‰) (Figure 7b). The addition of any land-derived DON inshore would tend to lower the $\delta^{15}N_{TDN}$ [*Guo and Macdonald*, 2006], which implies that it is the reactive N pool (NH_4^+ + NO_3^-) that is increasingly ^{15}N-enriched inshore. Again, assuming a $\delta^{15}N_{DON}$ of 5‰ at station 106, the $\delta^{15}N$ of NO_3^- + NH_4^+ is then on the order of ~7.7‰, compared to 6.5‰ for the NO_3^- off-shelf (Figure S4 in Text S1). Given the low $\delta^{15}N_{NO3}$ of 4.4‰ at this station, NH_4^+ (with a derived $\delta^{15}N_{NH4}$ of ~20‰) must drive this ^{15}N-enrichment of the reactive N pool. The net $\delta^{15}N$ elevation of the reactive N pool (NO_3^- + NH_4^+) then implies that the NH_4^+ ^{15}N-enrichment does not result solely from nitrification because the latter can only explain the $\delta^{15}N$ difference between water column NH_4^+ and NO_3^-, but does not affect the N-weighted $\delta^{15}N$ of NO_3^- + NH_4^+. To explain this ^{15}N-enrichment, we require the loss of low $\delta^{15}N$ reactive N from the water column, presumably to the sediment. Given that no diagenetic offset is expected from ammonification in sediment [*Prokopenko et al.*, 2006; *Velinsky et al.*, 1991], we must look to other processes to explain this. The association of greater $\delta^{15}N_{TDN}$ with N* (Figure 7b) suggests that the enrichment inshore derives from benthic denitrification.

[32] In the case of oxygenated bottom waters, NO_3^- produced by nitrification in the shallow sediments can subsequently become a substrate for sedimentary denitrification in the underlying suboxic sediments [*Christensen et al.*, 1987; *Devol*, 1991; *Devol and Christensen*, 1993; *Jahnke and Jahnke*, 2000; *Seitzinger*, 1988]. Sedimentary nitrification

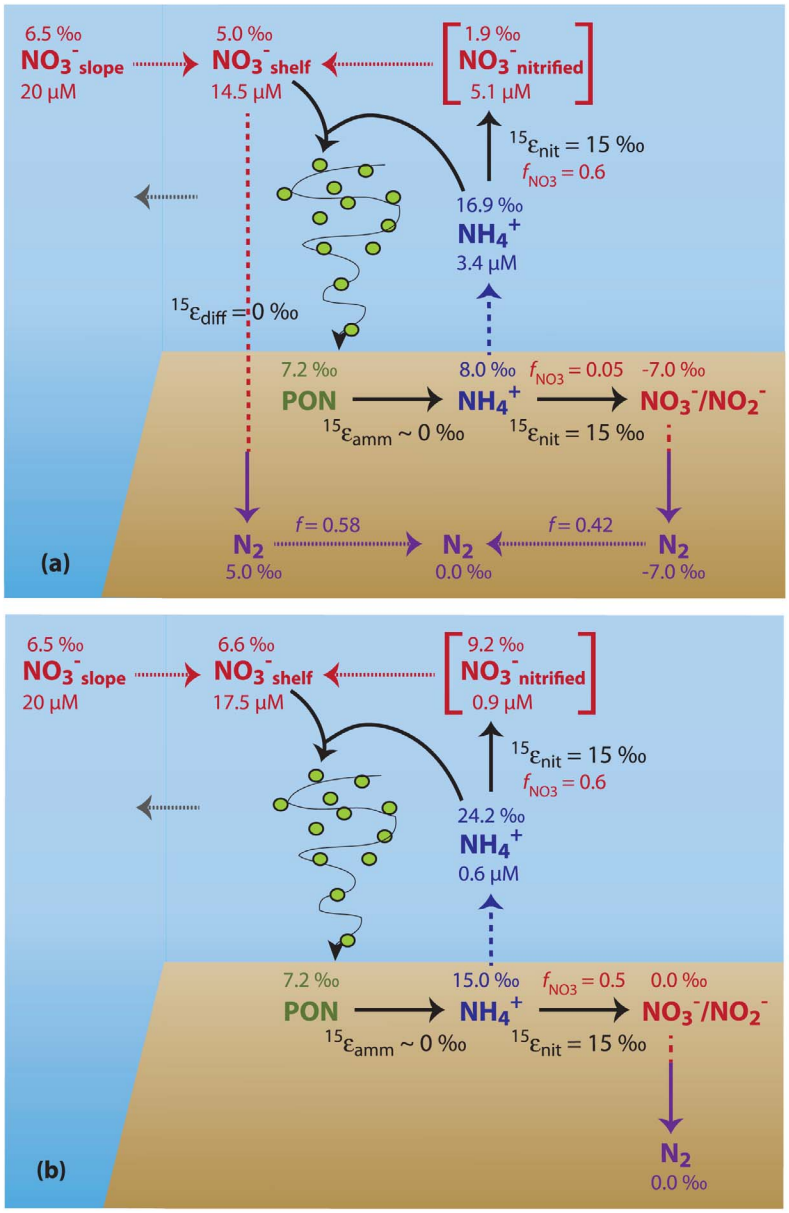

Figure 8

can reportedly contribute an equal or greater amount of oxidized nitrogen to the sediment pore water column than diffusion of NO_3^- from overlying waters, at times contributing up to 100% of the nitrate oxidant [*Laursen and Seitzinger*, 2002; *Lehmann et al.*, 2004].

[33] Our data and previous nutrient measurements demonstrate that the Bering Shelf hosts substantial NH_4^+ production from the seabed that is not perfectly coupled to the nitrification process [*Henriksen et al.*, 1993; *Lomstein et al.*, 1989; *Rowe and Phoel*, 1992; *Whitledge et al.*, 1986]. Given this imperfect coupling, partial nitrification of NH_4^+ in surface sediments will provide a ^{15}N-deplete NO_3^- substrate to underlying denitrification. In the context of a mass balance, the loss of ^{15}N-deplete NO_3^- as N_2 in sediment will then confer a net ^{15}N-enrichment to the reactive N species in shelf waters. ^{15}N-enrichment of the reactive N in the water column results proximally from the release of NH_4^+ that is ^{15}N-enriched due to benthic nitrification, occurring concurrently with the underlying denitrification that consumes the ^{15}N-deplete nitrate produced by benthic nitrification (Figure 8a). This dynamic has been observed in core incubations and benthic chambers on the Washington continental margin [*Brandes and Devol*, 1997]: An efflux of ^{15}N-enriched NH_4^+ was accompanied by the concomitant release of ^{15}N-deplete N_2 that was ~2‰ lower than the δ^{15}N of the organic N deposited on sediment, thus leading to a small net enrichment of the total reactive N pool in the overlying water ($\delta^{15}N_{rN}$).

[34] Notably, this mechanism of isotope fractionation associated with reactive N loss does not include a role for isotope discrimination by denitrifiers. This is consistent with the observed lack of ^{18}O-enrichment in winter-water NO_3^- (Figure 4c): ^{18}O-enrichment would be expected if the organism-level N and O isotope discrimination of NO_3^- by denitrifiers were communicated from the sediment depth of denitrification to the water column [*Granger et al.*, 2008; *Lehmann et al.*, 2004]. Strikingly, $\delta^{18}O_{NO3}$ in winter water correlates strongly with the extent of N loss to sedimentary denitrification, with lower $\delta^{18}O_{NO3}$ values corresponding to more negative N* values (Figure 9). This corroborates the notion that remineralization and denitrification on the shelf are linked mechanistically, wherein denitrification is fuelled by benthic nitrification. The correlation of $\delta^{18}O_{NO3}$ to N* further supports the hypothesis that the observed ^{15}N-enrichment of reactive N on the shelf results from the efflux of high-δ^{15}N NH_4^+ from surface sediment, and not from efflux of ^{15}N-enriched NO_3^- that had undergone partial denitrification in the sediments. In the latter case, winter NO_3^- would also be ^{18}O-enriched.

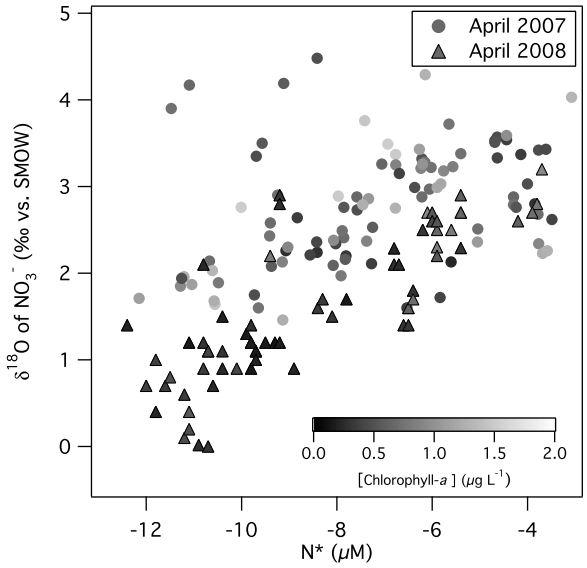

Figure 9. The $\delta^{18}O_{NO3}$ versus N* per ambient chlorophyll-*a* concentration in April 2007 and April 2008. The data are restricted to samples bearing no evidence of incident phytoplankton growth (chlorophyll-*a* concentration $\leq$1.6 μg L^{-1}; [O_2] $\leq$ 380 μM).

Figure 8. Conceptual steady state models of N isotope cycling between the sediment and the water column of the Bering Sea shelf. NO_3^- is continually mixed onto the shelf at the shelf edge from an infinite pool at 20 μM and a δ^{15}N of 6.5‰, while the steady state N pool in the shelf water column (18 μM NO_3^- + NH_4^+ with a δ^{15}N of 7.2‰) is concurrently mixed out. The steady state N loss to denitrification on-shelf is thus 10%. Particulate organic nitrogen (PON) derives from the complete assimilation of both NO_3^- and NH_4^+ in the growing season, and is ^{15}N-enriched ($\delta^{15}N_{PON}$ = 7.2‰) relative to NO_3^- off-shelf (6.5‰) due to benthic denitrification. The isotope enrichment of 0.7‰ associated with the 10% N loss corresponds to a shelf-wide isotope effect, $^{15}\varepsilon_{sed}$, of 7.2‰. PON deposited on sediment is completely ammonified with no associated N isotope discrimination ($^{15}\varepsilon_{amm}$ = 0‰). (a) Isotope effect of benthic denitrification, $^{15}\varepsilon_{sed}$, driven by both direct denitrification and coupled nitrification-denitrification. Of the NH_4^+ generated in sediment by the ammonification of PON, 5% is nitrified directly in surface sediment with an isotope effect, $^{15}\varepsilon_{nit}$, of 15‰, while 95% escapes to the water column. NO_3^- in surface sediment provides an oxidant for underlying sedimentary denitrification, resulting in a net loss of fixed N to N_2 with a $\delta^{15}N_2$ of −7‰. Of the NH_4^+ released to water column, 60% is nitrified directly to NO_3^- with a $^{15}\varepsilon_{nit}$ of 15‰, yielding relatively ^{15}N-deplete NO_3^- ($\delta^{15}N\ NO_{3nitrified}^-$ = 1.9‰). The combined steady state pool of shelf NO_3^- that derives from NO_3^- off-shelf and from newly nitrified NO_3^- is thus ^{15}N-deplete ($\delta^{15}N\ NO_{3shelf}^-$ = 5‰) relative to off-shelf. Denitrification is concurrently fuelled by direct NO_3^- diffusion into sediment, which has no associated isotope effect on NO_3^- ($^{15}\varepsilon_{diff}$ = 0‰), thus generating N_2 with the δ^{15}N of water column NO_3^- (5‰). The N_2 generated by both direct denitrification and coupled nitrification-deitrification has a net $\delta^{15}N_{N2}$ of 0‰, consistent with the $^{15}\varepsilon_{sed}$ of 7.2‰. (b) Isotope effect of benthic denitrification, $^{15}\varepsilon_{sed}$, mediated entirely by coupled nitrification-denitrification. Of the NH_4^+ generated by the ammonification of PON in sediment, 50% is shunted to coupled nitrification-denitrification, yielding N_2 with a $\delta^{15}N_{N2}$ of 0‰, which accounts for the shelf-wide $^{15}\varepsilon_{sed}$ of 7.2‰. An equivalent flux of NH_4^+ is released to the water column, of which 60% is nitrified to NO_3^- that is ^{15}N-enriched ($\delta^{15}N\ NO_{3nitrified}^-$ = 9.2‰) relative to NO_3^- off-shelf. Consequently, in this case shelf NO_3^- is ^{15}N-enriched ($\delta^{15}N\ NO_{3shelf}^-$ = 6.6‰) relative to off-shelf, violating these observations.

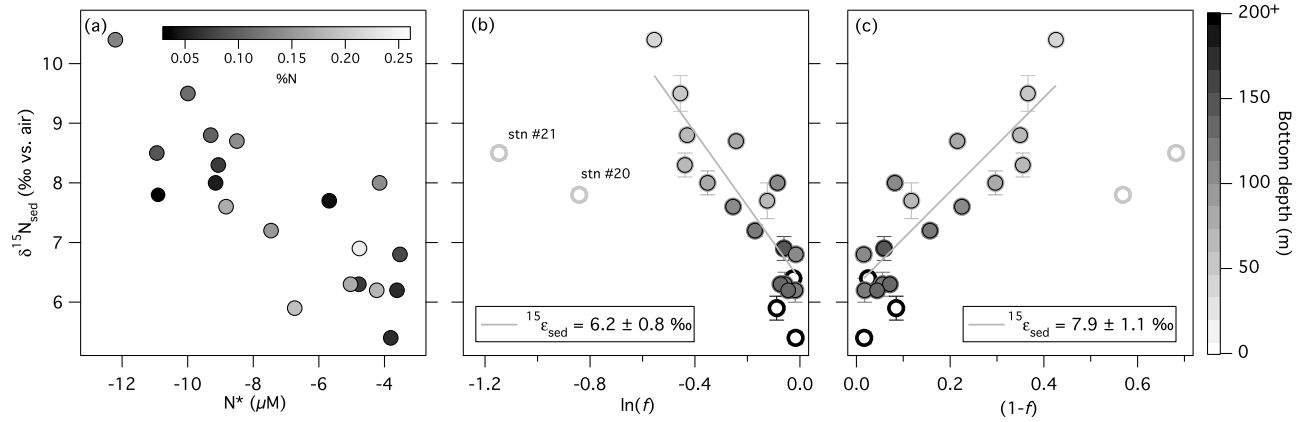

Figure 10. (a) The δ^{15}N of surface sediment versus N* in the overlying water column per of the sediment N content (%). (b) Closed Rayleigh model estimate of the N isotope effect associated with sedimentary N loss ($^{15}\varepsilon_{sed}$) on the eastern Bering Sea shelf: $\delta^{15}N_{sed}$ versus ln(f), where f = ([NO_3^-] +[NO_2^-] + [NH_4^+])/([NO_3^-] +[NO_2^-] + [NH_4^+] − ΔN*). $^{15}\varepsilon_{sed}$ = 6.2 ± 0.8‰, determined from the slope ± 1σ of the fitted linear regression; $\delta^{15}N_{initial}$ = 6.4 ± 0.2‰, corresponds to the intercept of the fitted linear regression. (c) Open model estimate of $^{15}\varepsilon_{sed}$: $\delta^{15}N_{sed}$ versus (1-f). $^{15}\varepsilon_{sed}$ = 7.9 ± 1.1 ‰; $\delta^{15}N_{initial}$ = 6.3 ± 0.3‰. The open symbols designate data omitted from the regression analyses for stations off-shelf and for apparent outliers (stations 20 and 21).

5.4. ^{15}N-Enrichment of Surface Sediment on the Shelf

[35] The spatial distribution of surface sediment δ^{15}N ($\delta^{15}N_{sed}$) offers additional evidence that, as reactive N is lost from the shelf, the remaining reactive N becomes ^{15}N-enriched compared to the $\delta^{15}N_{NO3}$ off-shelf (Figure 5). As with the measurements of $\delta^{15}N_{TDN}$, the $\delta^{15}N_{sed}$ of the middle and inner shelf regions was significantly greater than at the outer shelf region, 6.8‰ to 10.4‰ compared to 6.2‰ to 6.9‰ along the outer shelf. A similar pattern was noted by *Smith et al.* [2002] on the southern shelf, where the $\delta^{15}N_{sed}$ was 7.6‰ and 6.7‰ at the M2 and M4 moorings on the middle shelf, respectively, compared to 6.7‰ at the M3 mooring on the outer shelf (Figure 5). The greater $\delta^{15}N_{sed}$ at M2 was explained by either (1) more complete N utilization in summertime shelf surface waters than over the outer shelf region of M3, or (2) productivity over the middle and inner shelf associated with a contribution of heavy N from sediment regeneration [*Smith et al.*, 2002]. Incomplete N utilization does characterize the off-shelf surface waters, [*Aguilar-Islas et al.*, 2007], and may thus contribute to the lower $\delta^{15}N_{sed}$ of our most off-shelf samples (Figure 5). However, most of the sediment samples are from sites where reactive N is completely consumed during the summer, such that variation in the degree of N utilization by phytoplankton cannot explain most of the $\delta^{15}N_{sed}$ variation.

[36] Because of the complete consumption of NO_3^- and NH_4^+ in shelf surface waters during the growing season [*Sambrotto et al.*, 1986], the δ^{15}N of the sinking flux recorded in surface sediment ($\delta^{15}N_{sed}$) should reflect that of the reactive N pool ($\delta^{15}N_{rN}$) in the mixed layer. Thus, the geographic distribution of $\delta^{15}N_{sed}$ over the shelf suggests that the reactive N pool becomes progressively enriched in ^{15}N inshore from the shelf edge (Figure 5). Remarkably, the $\delta^{15}N_{sed}$ is highly correlated with the corresponding sedimentary N loss on the shelf, as quantified by N* (Figure 10a). This relationship strongly suggests that the loss of ^{15}N-deplete fixed N as N_2 during nitrification-coupled denitrification in sediment leads to, on a long-term average basis, higher $\delta^{15}N_{rN}$, and thus higher $\delta^{15}N_{sed}$ eastward and northward on the Bering shelf.

[37] The $\delta^{15}N_{sed}$ from Anadyr Straight and from the region north of St-Lawrence Island is also high, upwards of 11‰ through to Bering Straight [*Walsh et al.*, 1989]. This is consistent with the ^{15}N-enrichment of Bering shelf waters moving northward to the straight, and further suggests that coupled nitrification-denitrification is active in the sediment of the Anadyr region. Moreover, a survey of the δ^{15}N of copepods, euphausiids and chaetoghaths throughout the Bering Sea and the western Arctic showed clear ^{15}N-enrichment on the shelf shoreward and northward of the shelf break [*Schell et al.*, 1998]; the δ^{15}N of copepods at the surface of the open Bering Sea averaged ≤6‰, increasing to 8–10‰ on the southern shelf, and reached upwards of 14‰ near Bering Strait.

[38] One alternative hypothesis for the $\delta^{15}N_{sed}$ pattern across the Bering shelf is that sediment δ^{15}N is elevated variably by sedimentary diagenesis. This interpretation is discouraged by the lack of correlation to sediment N content (Figure 10a). Consistent with the lack of a major role for diagenesis, the sediment N content is roughly threefold higher than in the open ocean sediments where diagenesis has been observed to elevate the $\delta^{15}N_{sed}$ [*Galbraith et al.*, 2008]. A second alternative hypothesis is that organic matter associated with sea ice, which has been observed to have a high δ^{15}N [*Rau et al.*, 1991], is more important in the sediments to the east and north on the shelf, consistent with the extent and duration of annual sea ice cover (Figure S1 in Text S1). However, the organic N from sea ice probably does not represent a substantial fraction of the organic matter flux to the seabed given the shelf's dramatic water column algal bloom in the spring to summer. Finally, the riverine input of particulate organic N does not appear to account for the apparent ^{15}N-enrichment of surface sediment, as the $\delta^{15}N_{sed}$ throughout the Yukon River plume is ^{15}N-deplete compared

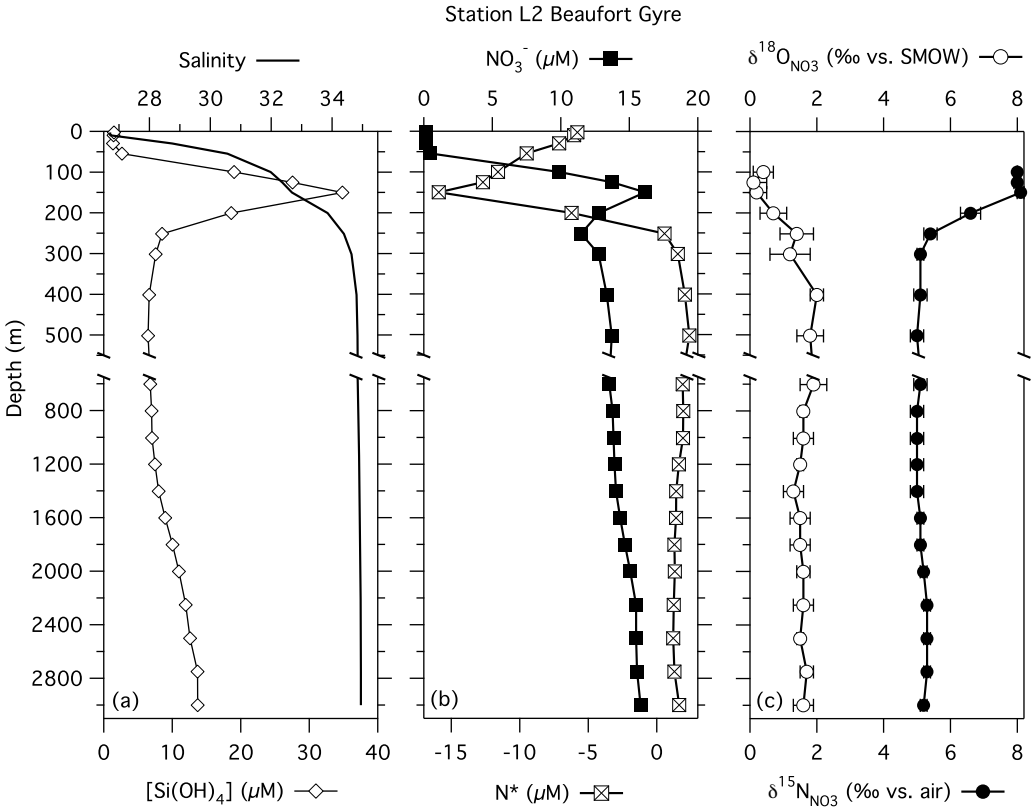

Figure 11. Chemical properties of the water column at station L2 (137.12 °W, 74.59 °N) in the Beaufort Gyre in the Arctic Ocean in August 2009. (a) Depth profiles of salinity and $[Si(OH)_4]$. (b) Depth profiles of $[NO_3^-]$ and N*. (c) Depth profiles of $\delta^{15}N_{NO3}$ and $\delta^{18}O_{NO3}$ ($\pm 1\sigma$).

to sediment outside of river influence, as low as 4‰ at the mouth of the river [*Walsh et al.*, 1989]. Indeed, the processes driving the $\delta^{15}N_{sed}$ increase toward the inner shelf must overcome the coastal sources of low-δ^{15}N organic matter; the concentration of DON in discharge from the Yukon is relatively high, with an inter-annual mean of 27 μM, while its δ^{15}N is reportedly low, around −1‰ [*Guo and Macdonald*, 2006]. Future work will investigate the importance of DON to the shelf N budget, particularly in light of increased delivery of land-derived organic N expected from enhanced permafrost thaw [*Davidson and Janssens*, 2006; *Frey et al.*, 2007; *Schuur et al.*, 2009].

[39] The evidence for an increase in the δ^{15}N of reactive N over the shelf leads to the prediction that the fixed N of Pacific provenance that is exported into the Arctic Ocean through Bering Strait will be enriched in ^{15}N relative to that of the open Bering Sea. Measurements of the $\delta^{15}N_{NO3}$ at an ice-covered station in the Beaufort Gyre in the Arctic Ocean appear to confirm this prediction (Figure 11). The nutrient concentration maximum observed in the halocline of the western Arctic is comprised mostly of nutrients of Pacific provenance that are delivered through Bering Strait and regenerated on the Arctic continental shelves [*Jones and Anderson*, 1986]. A distinct maximum in the $\delta^{15}N_{NO3}$ is associated with the NO_3^- maximum in the halocline, as high as 8‰ compared to 5‰ for NO_3^- of Atlantic provenance in the underlying water column. A coincident decrease in the $\delta^{18}O_{NO3}$ toward the top of the halocline confirms that NO_3^- at these depths is newly regenerated, such that the ^{15}N-enrichment of NO_3^- in the halocline does not reflect recent algal assimilation, which would lead to a parallel ^{18}O-enrichment of NO_3^- [*Granger et al.*, 2004]. The ^{15}N-elevating processes identified on the Bering shelf may well also occur on the Arctic shelves. However, the strong coincidence of our profile's nitrate δ^{15}N increase with tracers of Pacific water input to the Arctic (e.g., the $[NO_3^-]$ and $[Si(OH)_4]$ maxima, Figure 11) suggest that the Bering shelf is the major contributor of this signal.

5.5. N Isotope Effect of Coupled Nitrification-Denitrification in Bering Shelf Sediment

[40] As a first step toward evaluating the significance of the observed ^{15}N-enrichment of water column reactive N over the Bering shelf, we compare the bulk sediment $\delta^{15}N_{sed}$ data to the water column reactive N deficit to estimate the N isotope effect imposed by coupled nitrification-denitrification ($^{15}\varepsilon_{sed}$). The isotope effect is defined as $^{15}\varepsilon_{sed}$(‰) = ($^{14}k/^{15}k - 1$) * 1000, where ^{14}k and ^{15}k represent the rate constants for the light and heavy isotopologues of N, respectively. The estimate of $^{15}\varepsilon_{sed}$ roughly reflects the difference between the δ^{15}N of all reactive N in the water column ($\delta^{15}N_{rN}$) and the δ^{15}N of N_2 generated by denitrification in underlying sediment. In one scenario, the value of $^{15}\varepsilon_{sed}$ can be computed from the Rayleigh model, which assumes that denitrification acts on a finite fixed N pool that is not being replenished (i.e., a closed system), and the $\delta^{15}N_{sed} = \delta^{15}N_{initial} - {}^{15}\varepsilon_{sed} * \ln(f)$ [see *Hayes*, 2004]. The variable 'f' is the fraction of reactive N remaining in the

water column. '*f*' is calculated here from the sum of the inorganic N species measured in the water column ([NO_3^-], [NO_2^-], [NH_4^+]), divided by the sum of inorganic N species plus the N lost to sedimentary denitrification (i.e., minus ΔN*). One simplification in this approach is that the mineralization of DON does not add substantially to the reactive N pool, a reasonable starting assumption for oceanic waters [*Hansell and Carlson*, 2001; *Knapp et al.*, 2005]. In the case of no diagenetic effect on the $\delta^{15}N_{sed}$, the regression's estimate of $\delta^{15}N_{initial}$ should approximate the $\delta^{15}N$ of NO_3^- off-shelf that advects onto the shelf.

[41] Treatment of the shelf as a closed system, however, is an end-member assumption, given the exchange of water between shelf domains as well as across latitudes. As a result of this exchange, Rayleigh analysis should yield a lower bound estimate of $^{15}\varepsilon_{sed}$. In the alternative "steady state" model, denitrification is assumed to act on a fixed N pool that is being replenished continually and homogeneously throughout the shelf. In this model, $\delta^{15}N_{sed} = \delta^{15}N_{initial} + {}^{15}\varepsilon_{sed}(1 - f)$ [see *Hayes*, 2004]. Evaluation of the data with the steady state model should tend toward an upper bound for $^{15}\varepsilon_{sed}$.

[42] Applying the Rayleigh model, a coherent linear fit is observed between $\delta^{15}N_{sed}$ and ln(*f*), save for two neighboring stations located at the inner shelf region near Nunivak Island, which lie distinctly below the regression (Figure 10b). The two anomalous stations are located in a particularly fresh lens of water (Figure S2 in Text S1) that may be an advective plume of the Kuskokwim River [*Danielson et al.*, 2011], potentially explaining the apparent misfit. If these stations are excluded, the regression yields a $^{15}\varepsilon_{sed}$ of 6.2 ± 0.8‰. The intercept $\delta^{15}N_{initial}$ is 6.4 ± 0.2‰, consistent with the $\delta^{15}N_{NO3}$ observed at the shelf break. As expected, the alternate estimate of $^{15}\varepsilon_{sed}$ derived from the open system model is greater, with a slope of 7.9 ± 1.1‰ and an intercept of 6.3 ± 0.3‰ (Figure 10c).

[43] Additional uncertainty in the estimate of $^{15}\varepsilon_{sed}$ may arise from differences in the respective time scales captured by the $\delta^{15}N_{sed}$ and the water column nutrients. The $\delta^{15}N_{sed}$ is the annually integrated $\delta^{15}N$ of particles deposited on sediment, whereas nutrient concentrations, from which '*f*' is derived, reflect shelf processes that vary seasonally and inter-annually. While it is not clear that such discordance in time scales would lead to an estimate of $^{15}\varepsilon_{sed}$ that is considerably different from its true value, as N* does not appear to vary considerably inter-seasonally (Figure S5 in Text S1), the possibility cannot be discounted. In any case, the 4‰ increase in the $\delta^{15}N_{sed}$ observed over the shelf speaks of an important ^{15}N-enrichment of fixed N associated with shelf N loss.

5.6. Comparison to Previous Estimates of $^{15}\varepsilon_{sed}$

[44] The substantial amplitude of our estimate of $^{15}\varepsilon_{sed}$ is in contrast to previous reports of little to no isotope discrimination communicated to the water column by sedimentary N loss on either the Washington continental shelf or in the deep Bering Sea [*Brandes and Devol*, 1997; *Lehmann et al.*, 2007]. In the deep Bering Sea, the lack of significant isotope enrichment is explained by the associated mechanism of fixed N loss from sediment. Sedimentary denitrification in cores retrieved from the deep Bering Sea appears to be fuelled largely by the direct diffusion of water column NO_3^- into sediment [*Lehmann et al.*, 2007], which results in little to no isotope enrichment of the water column NO_3^- [*Brandes and Devol*, 1997; *Lehmann et al.*, 2004]. Additionally, efflux of ^{15}N-enriched NH_4^+ from open ocean deep sea sediment is expected to be minor, as NH_4^+ oxidation is virtually complete [*Berelson et al.*, 1990; *Lehmann et al.*, 2007].

[45] The likely cause for the difference in $^{15}\varepsilon_{sed}$ between the Bering and Washington shelves requires more consideration. On the Washington continental shelf, only a modest ^{15}N-enrichment was communicated from the sediment to the water column ($^{15}\varepsilon_{sed} \leq 2$‰). The existence of any fractionation at all appears to derive from the efflux of ^{15}N-enriched NH_4^+, due to partial nitrification of the NH_4^+ generated in sediment and to apparently complete denitrification of the resulting NO_2^- and NO_3^- [*Brandes and Devol*, 1997; *Lehmann et al.*, 2004]. Nearly half of the N_2 generated in sediment derived from coupled nitrification-denitrification in association with a corresponding efflux of high $\delta^{15}N$ NH_4^+. The 'gross' $^{15}\varepsilon_{sed}$ imprint of NH_4^+ efflux to the system was ~4‰. Concurrently, slightly more than 50% of denitrification in the Washington shelf sediments was fuelled directly by the influx of water column NO_3^-, which itself led to minimal ^{15}N-enrichment of the residual water column NO_3^-. The resulting 'net' $^{15}\varepsilon_{sed}$ (from both direct denitrification and nitrification-coupled denitrification) was thus ≤2‰.

[46] The Bering shelf is likely to be distinguished from the Washington shelf by a greater efflux of NH_4^+ from the sediment [*Henriksen et al.*, 1993; *Lomstein et al.*, 1989]. If coupled nitrification-denitrification is incomplete, that is, a substantial fraction of the remineralized NH_4^+ escapes to the overlying waters, then sedimentary N loss should be associated with a substantial $^{15}\varepsilon_{sed}$. This process may explain the high apparent $^{15}\varepsilon_{sed}$ of the Bering shelf, as illustrated in the following example.

[47] N transformations on the Bering shelf can be conceptualized with a steady state model of the shelf isotope mass balance (Figure 8a). We adopt a value of 15‰ for the isotope effect associated with nitrification of NH_4^+ to NO_3^- [*Casciotti et al.*, 2003] in both the water column and sediment, and prescribe an infinite NO_3^- source of 20 μM and 6.5‰ that mixes continually onto the shelf. Of the NH_4^+ flux in sediment arising from the degradation of PON, we test a scenario where 5% is shunted directly to coupled nitrification-dentirification while the remainder escapes to the water column. In and of itself, coupled nitrification-denitrification then communicates an isotope effect of 14.2‰ to shelf waters from the efflux of ^{15}N-enriched NH_4^+. However, in order to generate a shelf-wide ε_{sed} of 7.2‰, akin to that observed on the shelf (Figure 10), denitrification needs to be concomitantly fuelled by direct NO_3^- diffusion into sediments, which accounts for roughly half of the total benthic N loss in this example. The lack of isotope discrimination from direct denitrification dampens the large isotope effect of 14.2‰ communicated by coupled nitrification-denitrification, resulting in a "combined" apparent isotope effect of 7.2‰. The newly nitrified NO_3^- in the water column in this example has a relatively low $\delta^{15}N_{NO3}$, thus lowering the $\delta^{15}N_{NO3}$ of shelf NO_3^- compared off-shelf, which is analogous to our data (Figure 4a). Expectedly, the ^{15}N-enrichment associated benthic N loss ($^{15}\varepsilon_{sed}$ = 7.2‰) is manifested in

the δ^{15}N of sedimentary organic N, which is ^{15}N-enriched relative to off-shelf NO_3^-.

[48] An alternative means of "generating" a shelf-wide isotope effect of 7.2‰ in a steady state exercise is to assume that over 50% of the NH_4^+ in sediment is shunted directly to coupled nitrification-denitrification while 50% is released to the water column (Figure 8b). The N_2 thus generated is 7.2‰ lower than the fixed N on the shelf, such that coupled nitrification-denitrification single-handedly accounts for the shelf-wide $^{15}\varepsilon_{sed}$ of 7.2‰. However, the newly nitrified NO_3^- in the water column arising from this scenario is relatively ^{15}N-enriched, failing to reproduce the low $\delta^{15}N_{NO3}$ observed in situ. Regardless of the relative magnitude imposed on individual fluxes in this exercise, shelf NO_3^- maintains a $\delta^{15}N_{NO3}$ greater than, or equivalent to, NO_3^- off-shelf, in so far as the ratio of coupled nitrification-denitrification to NH_4^+ efflux remains relatively elevated. Therefore, the magnitude of $^{15}\varepsilon_{sed}$ manifested on the Bering shelf in light of the observed ^{15}N-deplete NO_3^- has two implications: (1) Both coupled nitrification-denitrification and direct denitrification are important mechanisms of fixed N loss on the shelf. (2) Only a small fraction of the NH_4^+ generated in sediment is shunted to coupled nitrification-denitrification, while the greater part escapes to the water column. On the Washington margin, while the fractional importance of direct denitrification to coupled nitrification-denitrification was comparable to that inferred for the Bering shelf, at least 50% of the NH_4^+ generated in sediment was shunted directly to coupled nitrification-denitrification [*Brandes and Devol*, 1997], consistent with the relatively lower isotope effect (~4‰) reported for this process.

5.7. Implications for the Global N Isotope Budget

[49] The $^{15}\varepsilon_{sed}$ derived from incubations of sediment on the Washington continental margin was ≤2‰, a value has been taken as representative of marine sediment denitrification globally [*Brandes and Devol*, 2002]. However, our estimate for the Bering shelf is substantially higher, and could be representative of other shallow and productive continental shelves. In particular, Arctic shelves are host to substantial benthic dentrification [*Brandes and Devol*, 1995; *Chang and Devol*, 2009; *Devol et al.*, 1997] and similarly exhibit benthic release of NH_4^+, facilitated by bioturbation and macrofaunal excretion [e.g., *Glud et al.*, 1998].

[50] On a global scale, it is unclear that benthic denitrification communicates significant isotope enrichment to the water column, particularly given that studies of the northeastern Pacific margin and of deep Bering Sea sediment argue for communication of a negligible isotope effect the water column [*Brandes and Devol*, 1997; *Lehmann et al.*, 2004, 2005, 2007]. The sensitivity of $^{15}\varepsilon_{sed}$ to various environmental factors was investigated by *Lehmann et al.* [2007] by extending a diagenetic model analysis of deep-sea sediment pore water constituents to simulate conditions characteristic of different sedimentary environments. While the model analysis diagnosed little to no isotope enrichment communicated to the water column by deep sea sediments, it forecast a $^{15}\varepsilon_{sed}$ of ~5‰ from reactive, well-oxygenated sediment, largely due to the efflux of ^{15}N-enriched NH_4^+ resulting from the nitrification component of the nitrification-denitrification couple. This prediction agrees remarkably well with our observations. Extrapolation of the model estimates of $^{15}\varepsilon_{sed}$ to different sedimentary environments further projected that sedimentary denitrification may be associated with a global mean $^{15}\varepsilon_{sed}$ of ~4‰ [*Lehmann et al.*, 2007].

[51] The possibility of a higher global $^{15}\varepsilon_{sed}$ than previously assumed adds new challenges to our current understanding of the global N isotope mass balance [*Brandes and Devol*, 2002]. Given a mean oceanic $\delta^{15}N_{NO3}$ of 5‰ [*Sigman et al.*, 2000], the flux-weighted inputs of fixed N to the ocean, which are dominated by biological N_2 fixation with a δ^{15}N of −1‰, must be balanced by flux-weighted losses that are on the order of ~6‰ lower than the inputs. Because water column denitrification is considered to occur with a disproportionately large isotope effect, ~25‰ [*Brandes et al.*, 1998; *Voss et al.*, 2001] the mean ocean NO_3^- δ^{15}N constraint would seem to require that most N loss occurs in the sediments, for which the effective isotope effect is less [*Brandes and Devol*, 2002; *Deutsch et al.*, 2004]. However, this analysis attributes a disproportionately larger fraction of N loss to sedimentary denitrification than is justified by current observations [*Brandes and Devol*, 2002; *Fennel et al.*, 2006]. Moreover, it yields an imbalanced N budget, with losses significantly in excess of the estimated global N_2 fixation rates [*Deutsch et al.*, 2007]. Yet, gross imbalances in the ocean's N inventory on centennial to millennial time scales are not borne out in the late Holocene sediment record [*Deutsch et al.*, 2004; *Ren et al.*, 2009]. If the average isotope effect for sedimentary denitrification is larger than previously assumed, as our data suggest, then the global fixed N budget appears even further out of balance. In our view, this result implies a fundamental error in our assumptions regarding the N isotope budget, but this error remains to be revealed. Further investigation of the controls on denitrification and its associated isotope dynamics in sediment and the water column is needed to resolve this paradox.

[52] **Acknowledgments.** We thank the captain and crew of the *U.S.C.G. Healy* and chief scientists Carin Ashjian and Evelyn Lessard. We are indebted to Boris Sirenko and Edward Davis for providing us with sediment core tops. Peter Proctor and Eric Wisegarver provided assistance with the nutrient analysis. CTD fluorometer data calibrated from discrete chlorophyll-*a* concentrations measured by Jeff Knapp (PMEL) in 2007 and Mike Lomas (BIOS) in 2008. Jonathan Gagnon and Jean-Eric Tremblay (U. Laval), and Roger François and Maureen Soon (UBC) provided samples and ancillary measurements from the Beaufort Sea during the Canadian IPY contribution to the International Geotraces Program aboard the *CCGS Louis St-Laurent* in August 2009. Sarah Fawcett, Bonnie Chang, Mathis Hain, and Katye Altieri provided comments on drafts of the manuscript, and Bror Johnson, Matt Long and Mathis Hain provided help with figures. Comments by two anonymous reviewers improved the manuscript. This research was funded by NSF's Office of Polar Programs as part of the Bering Ecosystem STudy (BEST) program (grants OPP-0612198 to DMS and OPP-0732430 and OPP-0813985 to CWM), with additional support from NSF grants OCE-0447570 and OPP-0453680 (DMS), the Siebel Energy Grand Challenge of Princeton University, the MacArthur Foundation, and the Joint Institute for the Study of the Atmosphere and Ocean (JISAO) under NOAA cooperative agreement NA17RJ1232, contribution 1831. This research is contribution 3623 to NOAA's Pacific Marine Environmental Laboratory, and contribution EcoFOCI-0758 to NOAA's Fisheries-Oceanography Coordinated Investigations. This research is contribution 25 to the BEST/BSIERP Bering Sea project.

References

Aguilar-Islas, A. M., M. P. Hurst, K. N. Buck, B. Sohst, G. J. Smith, M. C. Lohan, and K. W. Bruland (2007), Micro- and macronutrients in the southeastern Bering Sea: Insight into iron-replete and iron-depleted regimes, *Prog. Oceanogr.*, *73*, 99–126, doi:10.1016/j.pocean.2006.12.002.

Berelson, W. M., D. E. Hammond, D. O'Neill, X. M. Xu, C. Chin, and J. Zukin (1990), Benthic fluxes and pore water studies from sediments of the central equatorial N. Pacific: Nutrient diagenesis, *Geochim. Cosmochim. Acta*, *54*, 3001–3012, doi:10.1016/0016-7037(90)90117-4.

Böhlke, J. K., S. J. Mroczkowski, and T. B. Coplen (2003), Oxygen isotopes in nitrate: New reference materials for ^{18}O: ^{17}O: ^{16}O measurements and observations on nitrate-water equilibration, *Rapid Commun. Mass Spectrom.*, *17*, 1835–1846, doi:10.1002/rcm.1123.

Braman, R. S., and S. A. Hendrix (1989), Nanogram nitrite and nitrate determination in environmental and biological materials by vanadium (III) reduction with chemi-luminescence detection, *Anal. Chem.*, *61*, 2715–2718, doi:10.1021/ac00199a007.

Brandes, J. A., and A. H. Devol (1995), Simultaneous nitrate and oxygen respiration in coastal sediments—Evidence for discrete diagenesis, *J. Mar. Res.*, *53*, 771–797.

Brandes, J. A., and A. H. Devol (1997), Isotopic fractionation of oxygen and nitrogen in coastal marine sediments, *Geochim. Cosmochim. Acta*, *61*, 1793–1801, doi:10.1016/S0016-7037(97)00041-0.

Brandes, J. A., and A. H. Devol (2002), A global marine-fixed nitrogen isotopic budget: Implications for Holocene nitrogen cycling, *Global Biogeochem. Cycles*, *16*(4), 1120, doi:10.1029/2001GB001856.

Brandes, J. A., A. H. Devol, T. Yoshinari, D. A. Jayakumar, and S. W. A. Naqvi (1998), Isotopic composition of nitrate in the central Arabian Sea and eastern tropical North Pacific: A tracer for mixing and nitrogen cycles, *Limnol. Oceanogr.*, *43*, 1680–1689, doi:10.4319/lo.1998.43.7.1680.

Carpenter, J. H. (1965), The Chesapeake Bay Institute technique for the Winkler dissolved oxygen method, *Limnol. Oceanogr.*, *10*, 141–143, doi:10.4319/lo.1965.10.1.0141.

Casciotti, K. L., D. M. Sigman, M. G. Hastings, J. K. Böhlke, and A. Hilkert (2002), Measurement of the oxygen isotopic composition of nitrate in seawater and freshwater using the denitrifier method, *Anal. Chem.*, *74*, 4905–4912, doi:10.1021/ac020113w.

Casciotti, K. L., D. M. Sigman, and B. B. Ward (2003), Linking diversity and stable isotope fractionation in ammonia-oxidizing bacteria, *Geomicrobiol. J.*, *20*, 335–353, doi:10.1080/01490450303895.

Chang, B. X., and A. H. Devol (2009), Seasonal and spatial patterns of sedimentary denitrification rates in the Chuckchi Sea, *Deep Sea Res., Part II*, *56*, 1339–1350, doi:10.1016/j.dsr2.2008.10.024.

Christensen, J. P., W. M. Smethie, and A. H. Devol (1987), Benthic nutrient regeneration and denitrification on the Washington continental-shelf, *Deep Sea Res., Part A*, *34*, 1027–1047.

Clement Kinney, J., W. Maslowski, and S. Okkonen (2009), On the processes controlling shelf-basin exchange and outer shelf dynamics in the Bering Sea, *Deep Sea Res., Part II*, *56*, 1351–1362, doi:10.1016/j.dsr2.2008.10.023.

Coachman, L. K. (1982), Flow convergence over a broad, flat continental shelf, *Cont. Shelf Res.*, *1*, 1–14, doi:10.1016/0278-4343(82)90029-2.

Coachman, L. K. (1986), Circulation, water masses, and fluxes on the southeastern Bering Sea shelf, *Cont. Shelf Res.*, *5*, 23–108, doi:10.1016/0278-4343(86)90011-7.

Coachman, L. K., and R. L. Charnell (1979), Lateral water mass interaction—Case study, Bristol Bay, Alaska, *J. Phys. Oceanogr.*, *9*, 278–297, doi:10.1175/1520-0485(1979)009<0278:OLWMIC>2.0.CO;2.

Coachman, L. K., and J. J. Walsh (1981), A diffusion-model of cross-shelf exchange of nutrients in the southeastern Bering Sea, *Deep Sea Res., Part A*, *28*, 819–846.

Coachman, L. K., et al. (1975), *Bering Strait: The Regional Oceanography*, Univ. of Wash. Press, Seattle.

Cooper, L. W., G. F. Cota, L. R. Pomeroy, J. M. Grebmeier, and T. E. Whitledge (1999), Modification of NO, PO, and NO/PO during flow across the Bering and Chukchi shelves: Implications for use as Arctic water mass tracers, *J. Geophys. Res.*, *104*, 7827–7836, doi:10.1029/1999JC900010.

Danielson, S., K. Aagaard, T. Weingartner, S. Martin, P. Winsor, G. Gawarkiewicz, and D. Quadfasel (2006), The St. Lawrence polynya and the Bering shelf circulation: New observations and a model comparison, *J. Geophys. Res.*, *111*, C09023, doi:10.1029/2005JC003268.

Danielson, S., L. Eisner, T. Weingartner, and K. Aagaard (2011), Thermal and haline variability over the central Bering Sea shelf: Seasonal and interannual perspectives, *Cont. Shelf Res.*, *31*, 539–554, doi:10.1016/j.csr.2010.12.010.

Davidson, E. A., and I. A. Janssens (2006), Temperature sensitivity of soil carbon decomposition and feedbacks to climate change, *Nature*, *440*, 165–173, doi:10.1038/nature04514.

Deutsch, C., D. M. Sigman, R. C. Thunell, A. N. Meckler, and G. H. Haug (2004), Isotopic constraints on glacial/interglacial changes in the oceanic nitrogen budget, *Global Biogeochem. Cycles*, *18*, GB4012, doi:10.1029/2003GB002189.

Deutsch, C., J. L. Sarmiento, D. M. Sigman, N. Gruber, and J. P. Dunne (2007), Spatial coupling of nitrogen inputs and losses in the ocean, *Nature*, *445*, 163–167, doi:10.1038/nature05392.

Devol, A. H. (1991), Direct measurement of nitrogen gas fluxes from continental-shelf sediments, *Nature*, *349*, 319–321, doi:10.1038/349319a0.

Devol, A. H., and J. P. Christensen (1993), Benthic fluxes and nitrogen cycling in sediments of the continental margin of the eastern North Pacific, *J. Mar. Res.*, *51*, 345–372, doi:10.1357/0022240933223765.

Devol, A. H., L. A. Codispoti, and J. P. Christensen (1997), Summer and winter denitrification rates in western Arctic shelf sediments, *Cont. Shelf Res.*, *17*, 1029–1033, doi:10.1016/S0278-4343(97)00003-4.

Fennel, K., J. Wilkin, J. Levin, J. Moisan, J. O'Reilly, and D. Haidvogel (2006), Nitrogen cycling in the Middle Atlantic Bight: Results from a three-dimensional model and implications for the North Atlantic nitrogen budget, *Global Biogeochem. Cycles*, *20*, GB3007, doi:10.1029/2005GB002456.

Frey, K. E., J. W. McClelland, R. M. Holmes, and L. C. Smith (2007), Impacts of climate warming and permafrost thaw on the riverine transport of nitrogen and phosphorus to the Kara Sea, *J. Geophys. Res.*, *112*, G04S58, doi:10.1029/2006JG000369.

Fulweiler, R. W., S. W. Nixon, B. A. Buckley, and S. L. Granger (2007), Reversal of the net dinitrogen gas flux in coastal marine sediments, *Nature*, *448*, 180–182, doi:10.1038/nature05963.

Galbraith, E. D., D. M. Sigman, R. S. Robinson, and T. F. Pedersen (2008), Past changes in the marine nitrogen cycle, in *Nitrogen in the Marine Environment*, 2nd ed., edited by D. Capone et al., pp. 1497–1535, Academic, San Diego, Calif.

Glover, D. M., and W. S. Reeburgh (1987), Radon-222 and radium-226 in southeastern Bering Sea shelf waters and sediment, *Cont. Shelf Res.*, *7*, 433–456, doi:10.1016/0278-4343(87)90090-2.

Glud, R. N., O. Holby, F. Hoffmann, and D. E. Canfield (1998), Benthic mineralization and exchange in Arctic sediments (Svalbard, Norway), *Mar. Ecol. Prog. Ser.*, *173*, 237–251, doi:10.3354/meps173237.

Gonfiantini, R., W. Stichler, and K. Rosanski (1995), *Standards and Intercomparison Materials Distributed by the IAEA for Stable Isotope Measurements*, Int. At. Energy Agency, Vienna.

Gordon, L. I., et al. (1994), *WHP Operations and Methods*, WOCE Hydrogr. Program Off., La Jolla, Calif.

Granger, J., and D. M. Sigman (2009), Removal of nitrite with sulfamic acid for nitrate N and O isotope analysis with the denitrifier method, *Rapid Commun. Mass Spectrom.*, *23*, 3753–3762, doi:10.1002/rcm.4307.

Granger, J., D. M. Sigman, J. A. Needoba, and P. J. Harrison (2004), Coupled nitrogen and oxygen isotope fractionation of nitrate during assimilation by cultures of marine phytoplankton, *Limnol. Oceanogr.*, *49*, 1763–1773, doi:10.4319/lo.2004.49.5.1763.

Granger, J., D. M. Sigman, M. F. Lehmann, and P. D. Tortell (2008), Nitrogen and oxygen isotope fractionation during dissimilatory nitrate reduction by denitrifying bacteria, *Limnol. Oceanogr.*, *53*, 2533–2545, doi:10.4319/lo.2008.53.6.2533.

Grebmeier, J. M., L. W. Cooper, and M. J. Deniro (1990), Oxygen isotopic composition of bottom seawater and tunicate cellulose used as indicators of water masses in the northern Bering and Chukchi Seas, *Limnol. Oceanogr.*, *35*, 1182–1195, doi:10.4319/lo.1990.35.5.1182.

Grebmeier, J. M., J. E. Overland, S. E. Moore, E. V. Farley, E. C. Carmack, L. W. Cooper, K. E. Frey, J. H. Helle, F. A. McLaughlin, and S. L. McNutt (2006), A major ecosystem shift in the northern Bering Sea, *Science*, *311*, 1461–1464, doi:10.1126/science.1121365.

Gruber, N., and J. L. Sarmiento (1997), Global patterns of marine nitrogen fixation and denitrification, *Global Biogeochem. Cycles*, *11*, 235–266, doi:10.1029/97GB00077.

Guo, L. D., and R. W. Macdonald (2006), Source and transport of terrigenous organic matter in the upper Yukon River: Evidence from isotope ($\delta^{13}C$, $\Delta^{14}C$, and $\delta^{15}N$) composition of dissolved, colloidal, and particulate phases, *Global Biogeochem. Cycles*, *20*, GB2011, doi:10.1029/2005GB002593.

Guo, L. D., J. Z. Zhang, and C. Guegen (2004), Speciation and fluxes of nutrients (N, P, Si) from the upper Yukon River, *Global Biogeochem. Cycles*, *18*, GB1038, doi:10.1029/2003GB002152.

Haines, J. R., R. M. Atlas, R. P. Griffiths, and R. Y. Morita (1981), Denitrification and nitrogen fixation in Alaskan continental-shelf sediments, *Appl. Environ. Microbiol.*, *41*, 412–421.

Hansell, D. A., and C. A. Carlson (2001), Biogeochemistry of total organic carbon and nitrogen in the Sargasso Sea: Control by convective overturn, *Deep Sea Res., Part II*, *48*, 1649–1667, doi:10.1016/S0967-0645(00)00153-3.

Hansell, D. A., T. E. Whitledge, and J. J. Goering (1993), Patterns of nitrate utilization and new production over the Bering Chukchi shelf, *Cont. Shelf Res.*, *13*, 601–627, doi:10.1016/0278-4343(93)90096-G.

Hartnett, H. (1998), *Organic Carbon Input, Degradation and Preservation in Continental Margin Sediments: An Assessment of the Role of a Strong Oxygen Deficient Zone*, Univ. of Wash., Seattle.

Hayes, J. M. (2004), *An Introduction to Isotopic Calculations*, Woods Hole Oceanogr. Inst., Woods Hole, Mass.

Henriksen, K., T. H. Blackburn, B. A. Lomstein, and C. P. McRoy (1993), Rates of nitrification, distribution of nitrifying bacteria and inorganic N fluxes in northern Bering Chuckchi shelf sediments, *Cont. Shelf Res.*, *13*, 629–651, doi:10.1016/0278-4343(93)90097-H.

Hermann, A. J., et al. (2002), A regional tidal/subtidal circulation model of the southeastern Bering Sea: Development, sensitivity analyses and hindcasting, *Deep Sea Res., Part II*, *49*, 5945–5967, doi:10.1016/S0967-0645(02)00328-4.

Hoering, T. C., and H. T. Ford (1960), The isotope effect in the fixation of nitrogen by azotobacter, *J. Am. Chem. Soc.*, *82*, 376–378, doi:10.1021/ja01487a031.

Hunt, G. L., P. Stabeno, G. Walters, E. Sinclair, R. D. Brodeur, J. M. Napp, and N. A. Bond (2002), Climate change and control of the southeastern Bering Sea pelagic ecosystem, *Deep Sea Res., Part II*, *49*, 5821–5853, doi:10.1016/S0967-0645(02)00321-1.

Jahnke, R. A., and D. B. Jahnke (2000), Rates of C, N, P and Si recycling and denitrification at the US Mid-Atlantic continental slope depocenter, *Deep Sea Res., Part I*, *47*, 1405–1428, doi:10.1016/S0967-0637(99)00118-1.

Jones, E. P., and L. G. Anderson (1986), On the origin of the chemical properties of the Arctic Ocean halocline, *J. Geophys. Res.*, *91*, 759–767, doi:10.1029/JC091iC09p10759.

Jones, E. P., J. H. Swift, L. G. Anderson, M. Lipizer, G. Civitarese, K. K. Falkner, G. Kattner, and F. McLaughlin (2003), Tracing Pacific water in the North Atlantic Ocean, *J. Geophys. Res.*, *108*(C4), 3116, doi:10.1029/2001JC001141.

Kachel, N. B., G. L. Hunt, S. A. Salo, J. D. Schumacher, P. J. Stabeno, and T. E. Whitledge (2002), Characteristics and variability of the inner front of the southeastern Bering Sea, *Deep Sea Res., Part II*, *49*, 5889–5909, doi:10.1016/S0967-0645(02)00324-7.

Kinder, T. H., and L. K. Coachman (1978), Front overlaying continental slope in eastern Bering Sea, *J. Geophys. Res.*, *83*, 4551–4559, doi:10.1029/JC083iC09p04551.

Knapp, A. N., D. M. Sigman, and F. Lipschultz (2005), N isotopic composition of dissolved organic nitrogen and nitrate at the Bermuda Atlantic Time-series Study site, *Global Biogeochem. Cycles*, *19*, GB1018, doi:10.1029/2004GB002320.

Koike, I., and A. Hattori (1979), Estimates of denitrification in sediments of the Bering Sea shelf, *J. Geophys. Res.*, *26*, 409–415.

Laursen, A. E., and S. P. Seitzinger (2002), The role of denitrification in nitrogen removal and carbon mineralization in Mid-Atlantic Bight sediments, *Cont. Shelf Res.*, *22*, 1397–1416, doi:10.1016/S0278-4343(02)00008-0.

Lehmann, M. F., D. M. Sigman, and W. M. Berelson (2004), Coupling the $^{15}N/^{14}N$ and $^{18}O/^{16}O$ of nitrate as a constraint on benthic nitrogen cycling, *Mar. Chem.*, *88*, 1–20, doi:10.1016/j.marchem.2004.02.001.

Lehmann, M. F., D. M. Sigman, D. C. McCorkle, B. G. Brunelle, S. Hoffmann, M. Kienast, G. Cane, and J. Clement (2005), Origin of the deep Bering Sea nitrate deficit: Constraints from the nitrogen and oxygen isotopic composition of water column nitrate and benthic nitrate fluxes, *Global Biogeochem. Cycles*, *19*, GB4005, doi:10.1029/2005GB002508.

Lehmann, M. F., D. M. Sigman, D. C. McCorkle, J. Granger, S. Hoffmann, G. Cane, and B. G. Brunelle (2007), The distribution of nitrate $^{15}N/^{14}N$ in marine sediments and the impact of benthic nitrogen loss on the isotopic composition of oceanic nitrate, *Geochim. Cosmochim. Acta*, *71*, 5384–5404, doi:10.1016/j.gca.2007.07.025.

Lomstein, B. A., T. H. Blackburn, and K. Henriksen (1989), Aspects of nitrogen and carbon cycling in the northern Bering shelf sediment: 1. The significance of urea turnover in the mineralization of NH_4^+, *Mar. Ecol. Prog. Ser.*, *57*, 237–247.

Mantoura, R. F. C., and E. M. S. Woodward (1983), Optimization of the indophenol blue method for the automated-determination of ammonia in estuarine waters, *Estuarine Coastal Shelf Sci.*, *17*, 219–224, doi:10.1016/0272-7714(83)90067-7.

Mizobata, K., S. Saitoh, and J. Wang (2008), Interannual variability of summer biochemical enhancement in relation to mesoscale eddies at the shelf break in the vicinity of the Pribilof Islands, Bering Sea, *Deep Sea Res., Part II*, *55*, 1717–1728, doi:10.1016/j.dsr2.2008.03.002.

Nihoul, J. C. J., P. Adam, P. Brasseur, E. Deleersnijder, S. Djenidi, and J. Haus (1993), 3-dimensional general-circulation model of the northern Bering Seas summer ecohydrodynamics, *Cont. Shelf Res.*, *13*, 509–542, doi:10.1016/0278-4343(93)90093-D.

Prokopenko, M. G., et al. (2006), Nitrogen cycling in the sediments of Santa Barbara basin and eastern subtropical North Pacific: Nitrogen isotopes, diagenesis and possible chemosymbiosis between two lithotrophs (Thioploca and Anammox)—"Riding on a glider," *Earth Planet. Sci. Lett.*, *242*, 186–204, doi:10.1016/j.epsl.2005.11.044.

Rau, G. H., C. W. Sullivan, and L. I. Gordon (1991), $\delta^{13}C$ and $\delta^{15}N$ variations in Weddell Sea particulate organic matter, *Mar. Chem.*, *35*, 355–369, doi:10.1016/S0304-4203(09)90028-7.

Ray, G. C., J. McCormick-Ray, P. Berg, and H. E. Epstein (2006), Pacific walrus: Benthic bioturbator of Beringia, *J. Exp. Mar. Biol. Ecol.*, *330*, 403–419, doi:10.1016/j.jembe.2005.12.043.

Reed, R. K. (1998), Confirmation of a convoluted flow over the southeastern Bering sea shelf, *Cont. Shelf Res.*, *18*, 99–103, doi:10.1016/S0278-4343(97)00069-1.

Ren, H., D. M. Sigman, A. N. Meckler, B. Plessen, R. S. Robinson, Y. Rosenthal, and G. H. Haug (2009), Foraminiferal isotope evidence of reduced nitrogen fixation in the ice age Atlantic Ocean, *Science*, *323*, 244–248, doi:10.1126/science.1165787.

Rho, T. K., T. E. Whitledge, and J. J. Goering (2005), Interannual variations of nutrients and primary production over the southeastern Bering Sea shelf during the spring of 1997, 1998, and 1999, *Oceanology, Engl. Transl.*, *45*, 376–390.

Rowe, G. T., and W. C. Phoel (1992), Nutrient regeneration and oxygen demand in Bering Sea continental shelf sediments, *Cont. Shelf Res.*, *12*, 439–449, doi:10.1016/0278-4343(92)90085-X.

Sambrotto, R. N., H. J. Niebauer, J. J. Goering, and R. L. Iverson (1986), Relationships among vertical mixing, nitrate uptake, and phytoplankton growth during the spring bloom in the southeast Bering Sea middle shelf, *Cont. Shelf Res.*, *5*, 161–198, doi:10.1016/0278-4343(86)90014-2.

Schell, D. M., B. A. Barnett, and K. A. Vinette (1998), Carbon and nitrogen isotope ratios in zooplankton of the Bering, Chukchi and Beaufort Seas, *Mar. Ecol. Prog. Ser.*, *162*, 11–23, doi:10.3354/meps162011.

Schumacher, J. D., and T. H. Kinder (1983), Low-frequency current regimes over the Bering Sea shelf, *J. Phys. Oceanogr.*, *13*, 607–623, doi:10.1175/1520-0485(1983)013<0607:LFCROT>2.0.CO;2.

Schumacher, J. D., T. H. Kinder, D. J. Pashinski, and R. L. Charnell (1979), Structural front over the continental shelf of the eastern Bering Sea, *J. Phys. Oceanogr.*, *9*, 79–87, doi:10.1175/1520-0485(1979)009<0079:ASFOTC>2.0.CO;2.

Schuur, E. A. G., J. G. Vogel, K. G. Crummer, H. Lee, J. O. Sickman, and T. E. Osterkamp (2009), The effect of permafrost thaw on old carbon release and net carbon exchange from tundra, *Nature*, *459*, 556–559, doi:10.1038/nature08031.

Seitzinger, S. P. (1988), Denitrification in fresh-water and coastal marine ecosystems—Ecological and geochemical significance, *Limnol. Oceanogr.*, *33*, 702–724, doi:10.4319/lo.1988.33.4_part_2.0702.

Sigman, D., M. Altabet, D. McCorkle, R. Francois, and G. Fischer (2000), The $\delta^{15}N$ of nitrate in the Southern Ocean: Nitrogen cycling and circulation in the ocean interior, *J. Geophys. Res.*, *105*(C8), 19,599–19,614.

Sigman, D. M., K. L. Casciotti, M. Andreani, C. Barford, M. Galanter, and J. K. Böhlke (2001), A bacterial method for the nitrogen isotopic analysis of nitrate in seawater and freshwater, *Anal. Chem.*, *73*, 4145–4153, doi:10.1021/ac010088e.

Sigman, D. M., P. J. DiFiore, M. P. Hain, C. Deutsch, and D. M. Karl (2009), Sinking organic matter spreads the nitrogen isotope signal of pelagic denitrification in the North Pacific, *Geophys. Res. Lett.*, *36*, L08605, doi:10.1029/2008GL035784.

Smith, S. L., S. M. Henrichs, and T. Rho (2002), Stable C and N isotopic composition of sinking particles and zooplankton over the southeastern Bering Sea shelf, *Deep Sea Res., Part II*, *49*, 6031–6050, doi:10.1016/S0967-0645(02)00332-6.

Stabeno, P. J., and P. Van Meurs (1999), Evidence of episodic on-shelf flow in the southeastern Bering Sea, *J. Geophys. Res.*, *104*, 29,715–29,720, doi:10.1029/1999JC900242.

Stabeno, P. J., N. B. Kachel, M. Sullivan, and T. E. Whitledge (2002a), Variability of physical and chemical characteristics along the 70-m isobath of the southeastern Bering Sea, *Deep Sea Res., Part II*, *49*, 5931–5943, doi:10.1016/S0967-0645(02)00327-2.

Stabeno, P. J., R. K. Reed, and J. M. Napp (2002b), Transport through Unimak Pass, Alaska, *Deep Sea Res., Part II*, *49*, 5919–5930, doi:10.1016/S0967-0645(02)00326-0.

Stabeno, P. J., N. A. Bond, and S. A. Salo (2007), On the recent warming of the southeastern Bering Sea shelf, *Deep Sea Res., Part II*, *54*, 2599–2618, doi:10.1016/j.dsr2.2007.08.023.

Tanaka, T., L. D. Guo, C. Deal, N. Tanaka, T. Whitledge, and A. Murata (2004), N deficiency in a well-oxygenated cold bottom water over the Bering Sea shelf: Influence of sedimentary denitrification, *Cont. Shelf Res.*, *24*, 1271–1283, doi:10.1016/j.csr.2004.04.004.

Velinsky, D. J., M. L. Fogel, J. F. Todd, and B. M. Tebo (1991), Isotopic fractionation of dissolved ammonium at the oxygen-hydrogen sulfide

interface in anoxic waters, *Geophys. Res. Lett.*, *18*, 649–652, doi:10.1029/91GL00344.

Voss, M., J. W. Dippner, and J. P. Montoya (2001), Nitrogen isotope patterns in the oxygen-deficient waters of the eastern tropical North Pacific Ocean, *Deep Sea Res., Part I*, *48*, 1905–1921, doi:10.1016/S0967-0637(00)00110-2.

Walsh, J. J., and C. P. McRoy (1986), Ecosystem analysis in the southeastern Bering Sea, *Cont. Shelf Res.*, *5*, 259–288, doi:10.1016/0278-4343(86)90018-X.

Walsh, J. J., E. T. Premuzic, J. S. Gaffney, G. T. Rowe, G. Harbottle, R. W. Stoenner, W. L. Balsam, P. R. Betzer, and S. A. Macko (1985), Organic storage of CO_2 on the continental-slope off the Mid-Atlantic Bight, the southeastern Bering Sea, and the Peru coast, *Deep Sea Res., Part A*, *32*, 853–883.

Walsh, J. J., et al. (1989), Carbon and nitrogen cycling within the Bering Chukchi Seas—Source regions for organic matter effecting AOU demands of the Arctic Ocean, *Prog. Oceanogr.*, *22*, 277–359, doi:10.1016/0079-6611(89)90006-2.

Whitledge, T. E., W. S. Reeburgh, and J. J. Walsh (1986), Seasonal inorganic nitrogen distributions and dynamics in the southeastern Bering Sea, *Cont. Shelf Res.*, *5*, 109–132, doi:10.1016/0278-4343(86)90012-9.

Yamamoto-Kawai, M., E. Carmack, and F. McLaughlin (2006), Nitrogen balance and Arctic throughflow, *Nature*, *443*, 43–43, doi:10.1038/443043a.

J. Granger, Department of Marine Sciences, University of Connecticut, Groton, CT 06340, USA. (julie.granger@uconn.edu)

L. V. Morales, Z. M. Morse, and D. M. Sigman, Geosciences Department, Princeton University, Princeton, NJ 08544, USA.

C. W. Mordy, Joint Institute for the Study of the Atmosphere and Ocean, University of Washington, Seattle, WA 98105-5672, USA.

B. Plessen, Geoforschungszentrum Potsdam, D-14473, Potsdam, Germany.

M. G. Prokopenko, Department of Earth Sciences, University of Southern California, Los Angeles, CA 90089-0704, USA.

R. N. Sambrotto, Lamont-Doherty Earth Observatory, Earth Institute at Columbia University, Palisades, NY 10964, USA.